1. Report No. FHWA/TX-04/0-4404-2	2. Government Accession No.	3. Recipient's Catalog No.
4. Title and Subtitle MEASUREMENT AND SIMULATION OF FLOW ON SURFACES WITH EXTREME LOW SLOPE FOR DETERMINATION OF TIME OF CONCENTRATION		5. Report Date Resubmitted: May 2005
		6. Performing Organization Code
7. Author(s) Anthony Cahill and Ming-Han Li		8. Performing Organization Report No. Report 0-4404-2
9. Performing Organization Name and Address Texas Transportation Institute The Texas A&M University System College Station, Texas 77843-3135		10. Work Unit No. (TRAIS)
		11. Contract or Grant No. Project 0-4404
12. Sponsoring Agency Name and Address Texas Department of Transportation Research and Technology Implementation Office P. O. Box 5080 Austin, Texas 78763-5080		13. Type of Report and Period Covered Technical Report: September 2002 - August 2003
		14. Sponsoring Agency Code

15. Supplementary Notes
Project performed in cooperation with the Texas Department of Transportation and the Federal Highway Administration.
Project Title: Estimating Travel Time of Direct Runoff in Areas of Very Flat Terrain
URL: http://tti.tamu.edu/documents/0-4404-2.pdf

16. Abstract
Field laboratory experiments and numerical simulations were used to explore the question of estimating time of concentration for regions with negligible slope. Current methods for estimating time of concentration generally have the slope of the land surface in the denominator of the functional relationship. This means that as slope decreases to zero, the time of concentration becomes infinite, which is contrary to observations. Researchers performed a set of experiments with a rainfall simulator over beds of very low slope. The resulting hydrographs were used to determine the time of concentration as a function of the slope and other pertinent variables. A numerical model was also developed to simulate the flow of water over a low-slope surface with random microtopography. While the field measurements provided some successful insight, the results from the two approaches were not able to determine definitively a relationship for time of concentration that can be used in all cases. The field laboratory study may have suffered from being too small scale compared to the area of the watersheds (~100 Ac) for which time of concentration is sought. The numerical study suffered from instabilities brought about by the nature of the equations modeled and, possibly, from lack of knowledge about the boundary conditions. Based on the experience and knowledge gained from this work, it is recommended that future work to determine the time of concentration for regions of low slope would benefit from one or more field observation facilities, where rainfall and flow records could be measured. Additionally, because different times of concentrations were derived in this study depending on the flow conditions or time of concentration determination technique, a standard definition (or standard definitions) of time of concentration is needed.

17. Key Words Time of Concentration, Runoff Flow, Runoff Travel Time, Microtopography		18. Distribution Statement No restrictions. This document is available to the public through NTIS: National Technical Information Service Springfield, Virginia 22161 http://www.ntis.gov
19. Security Classif.(of this report) Unclassified	20. Security Classif.(of this page) Unclassified	21. No. of Pages 68 22. Price

Form DOT F 1700.7 (8-72)   Reproduction of completed page authorized

MEASUREMENT AND SIMULATION OF FLOW ON SURFACES WITH EXTREME LOW SLOPE FOR DETERMINATION OF TIME OF CONCENTRATION

by

Dr. Anthony Cahill
Assistant Professor
Civil Engineering, Texas A&M University

and

Dr. Ming-Han Li
Assistant Research Engineer
Texas Transportation Institute

Report 0-4404-2
Project 0-4404
Project Title: Estimating Travel Time of Direct Runoff in Areas of Very Flat Terrain

October 2003
Resubmitted: May 2005

TEXAS TRANSPORTATION INSTITUTE
The Texas A&M University System
College Station, Texas   77843-3135

DISCLAIMER

The contents of this report reflect the views of the authors, who are responsible for the facts and the accuracy of the data presented herein. The contents do not necessarily reflect the official view or policies of the Federal Highway Administration (FHWA) or the Texas Department of Transportation (TxDOT). This report does not constitute a standard, specification, or regulation. The researcher in charge was Anthony Cahill.

ACKNOWLEDGMENTS

TABLE OF CONTENTS

Page

LIST OF FIGURES

LIST OF TABLES

INTRODUCTION

The Texas Department of Transportation (TXDOT) is aware that current methods of estimating the time of concentration fail when applied to areas with very low slope. The reason for this problem is the appearance of the slope in the denominator of most expressions for predicting time of concentration. As the slope decreases to zero, the time of concentration increases to infinity, which is not borne out by observation. In order to develop new expressions for the estimation of time of concentration for areas with extremely low slope, a set of field laboratory experiments and numerical simulations was performed in order to provide data that could be used to develop a new relationship between the time of concentration and the traditional explanatory variables: slope, rainfall intensity, area, and surface roughness. These approaches were undertaken because of the lack of appropriate data needed for a more traditional regression approach.

This report contains the methods and results of both approaches as well as the shortcomings found in the line of attack on this problem. One primary discovery of both approaches is that the method of inducing the flow of water across the surface or the method of determining the time of concentration can produce significantly different values for the time of concentration. The implication of this finding is that researchers need guidance from TxDOT about what their definition of time of concentration is.

CHAPTER 1:
NUMERICAL EXPERIMENT

A numerical model of a low-slope flow system was developed by the researchers to allow simulation of sheet flow over the land surface. The overall slope of the land surface in the model could be set to a negligible number (<0.5 percent) to mimic the situation explored in the problem statement. The simulated land surface also incorporated microtopography, which allowed various simulation of surface roughnesses. Spatially variable rainfall and infiltration were also possible with the model, but these capabilities generally were not used in model runs because of a lack of information on realistic spatial variability. Because of the nature of the simulated flow system, the numerical system was highly unstable, limiting the number of successful simulations achieved. While these successful simulations provided, the difficulty in numerically modeling a shallow-slope overland flow system indicates that further physical experimentation is needed.

MODELING OF TWO-DIMENSIONAL OVERLAND FLOW

Rather than beginning with the Saint-Venant equations, or a further simplification of these equations such as the dynamic wave or Manning's equations, we developed our model from the Navier-Stokes equations. Although these equations are more complicated than the Saint-Venant equations (the Saint-Venant equations are a simplification of the Navier-Stokes equations), by using the complete Navier-Stokes equations we hoped to avoid some of the counter-intuitive results that result from using simpler flow models (i.e., the presence of the slope in the denominator of the equation for flow, which leads to infinite time of concentration when the slope is zero.)

Regardless of the equations chosen for the starting point for the model, the overland flow system under consideration presents a number of difficulties for numerical modeling:

- Overland flow is a free-surface flow, so the height of the upper boundary condition (the height of the water) must be calculated.
- Overland flow is very shallow, both in absolute terms and relative to the horizontal dimensions. Numerical oscillations in the computed height of the

water can be large relative to the height of the water. This can lead to the aphysical situation where the computed height of the water at some nodes is negative. When this occurs, the numerical simulation rapidly becomes unstable.

- The bed shear stress is large and must be effectively transmitted across the shallow water layer.
- The variation in the local slope gradient caused by the microtopography is also a significant driving force for the flow and must be carefully accounted for.
- Rainfall and infiltration are mathematically significant sources and sinks of mass and momentum, respectively.

For a shallow, free-surface flow, a recommended numerical method for treating the partial differential equations is a MacCormick finite difference system. This method attempts to minimize numerical instability by using a predictor-corrector scheme, which is made symmetric in space by reversing the x- and y-direction steps in each time step.

The bottom boundary shear stress is treated by using an equation that parameterizes the specific surface type with Manning's n. Manning's n varies from point to point in space, as the surface type varies. Slope is not used in this equation, which avoids the problem of calculating infinite time of concentration. The use of Manning's n to parameterize the surface roughness is still an approximation, however, and adds to the uncertainty of the results. There are, unfortunately, no straightforward means of treating the momentum transfer at the lower boundary that do not involve numerical modeling of the eddies smaller than the surface roughness scale. This level of numerical modeling would have been too great for the horizontal scale we wanted to model. (We would have spent so much computation time on the momentum transfer that we could have only done a very limited number of nodes in the horizontal direction.) Future numerical modeling work on this question should examine better means of parameterizing the bottom boundary momentum transfer.

MICROTOPOGRAPHY

One feature of the model developed for this project is the inclusion of microtopography in the surface model. Although a land surface may have negligible net surface slope, a surface roughness gives rise to local, small-scale slopes. These slopes can run in any direction, even counter to the large-scale slope for the area. Figure 1 illustrates this sort of microtopography. Even in a region that is flat overall (drawing left) surface roughness can give rise to local slope. The microtopography will exist even in areas with large-scale slope (drawing right).
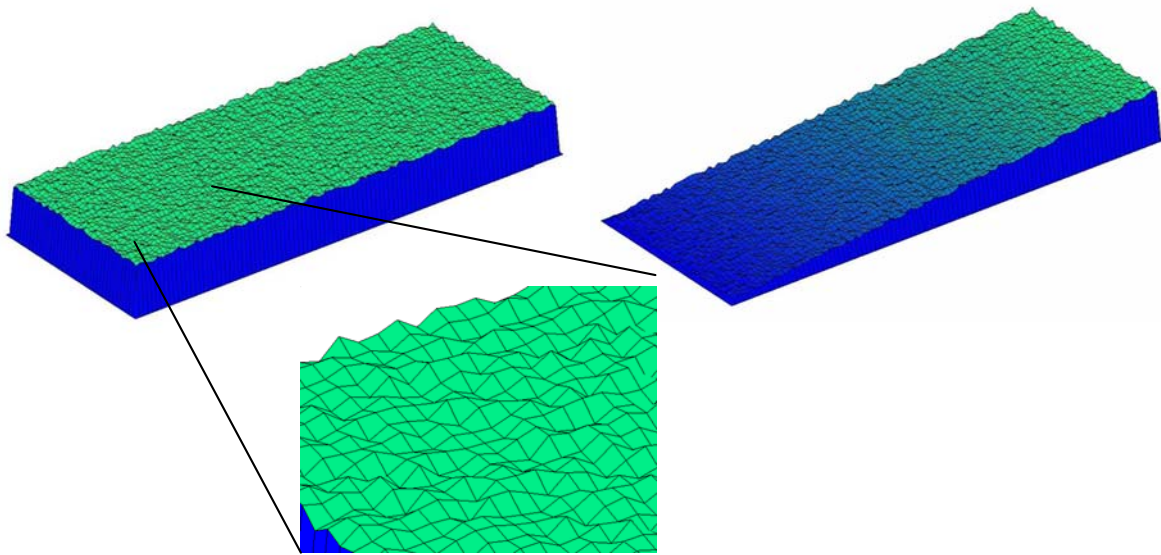
Figure 1. Schematic Drawing of Microtopography.

The arrangement of the microtopography in space has an important impact on the overall flow, since for shallow flows (flows with depths on the order of the roughness element height) the arrangement of small-scale slopes determines the flow speed, the amount of detention/ponding, and the connectivity of the flow (at least until the flow depth is greater than the roughness element height).

In the simulations, roughness element height was controlled by the variance of a zero mean Gaussian fluctuation around a mean plane that followed the large-scale slope. Any resulting negative surface heights were eliminated as unphysical. A Gaussian distribution of roughness was chosen because of the prevalence of Gaussian noise in

natural systems. Surface roughness measurements taken during the laboratory experiments were not used directly for the microtopography because they were taken on a larger scale (2.36 in) than the spacing of the numerical model (.394 in). The Gaussian distribution was supported by these measurements, however.

MODEL RUNS

Once the numerical code was developed and tested, a number of runs were performed. The parameters varied in the different runs were large-scale slope, roughness variance, and Manning's n. For each run, a new random surface roughness was generated using the roughness variance chosen. Manning's n was constant across the surface, as were infiltration and rainfall, because of a lack of information on what sort of spatial variation was realistic. Unfortunately, many combinations of parameters and surface roughnesses yielded an unstable numerical model that led to unrealistic flows. One of the major problems was the occurrence of negative flow depths, due to numerical fluctuation. In some instances, we were able to deal with this problem by reducing the time step in the numerical model to approximately 0.05 seconds, but this solution was not always possible. The failure of certain combinations of parameters and random surface roughnesses indicates that work is needed in both the numerical scheme used and in real-world observations. The use of an uncorrelated random surface may not be a realistic system; real surfaces may show spatial correlation of small-scale roughness, which is needed in the numerical model for stability. A better treatment of boundary layer shear stress than Manning's n might help the stability problems too, by better damping numerical oscillations.

A simulation run consisted of a defined surface, initial condition, and rainfall. The physical area simulated was an area close in size to that used in the field laboratory experiments: 30 ft by 6 ft. The spatial separation between calculation nodes was 1 cm. The primary type of run consisted of an initially almost-dry surface, with uniform rainfall beginning at time zero. (The surface was given an initial water depth of 0.00001 inches, in order to avoid a numerical singularity at time zero.) The rainfall rate was always chosen to be greater than the steady state infiltration rate, so that runoff would be generated. As the surface wetted, flow occurred, and eventually a steady-state velocity

6

map arose (figure 2). The distance between the center of each cell is known, and the model computes velocity of the flow between them. Travel time between the center of each cell is computed from distance and velocity, and then all travel times are summed to yield time of concentration.
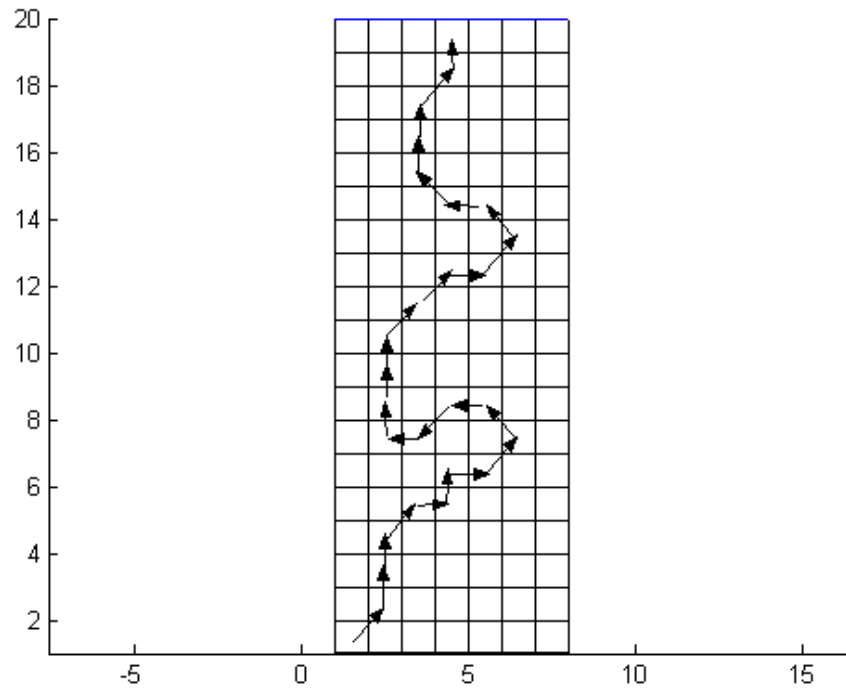

Figure 2. Flow velocity map for the determination of time of concentration.

Researchers calculated the volumetric flow at the outlet of the region through time and measured a simulated hydrograph.

Based on this simulation, the time of concentration could be calculated in two ways:

1. The first method was based on the definition of time of concentration as the time it takes water from the hydraulically most distant point to reach the outlet. From the flow velocity maps, the travel time from this most distant point to the outlet could be directly calculated by dividing the distance

7

between cells by the velocity between individual cells and then summing over the entire flow path (figure 3). Time of concentration (Tc) is defined as the time between the end of rain and the inflection point in the falling limb of the hydrograph.
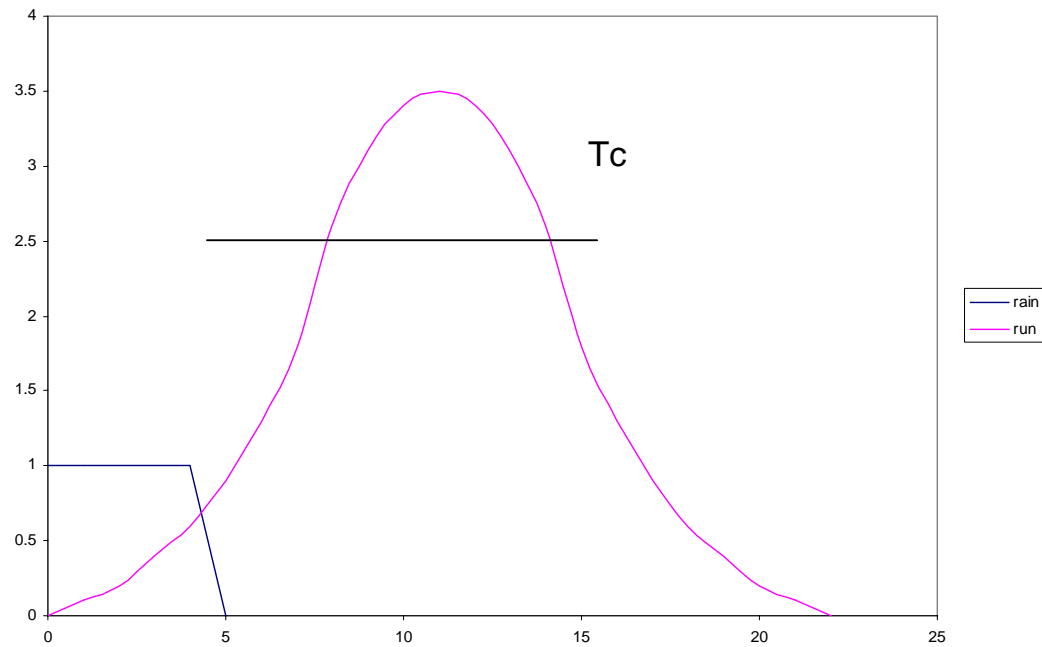
Figure 3. Time of Concentration Determined by Hydrograph Method.

2. The second method was based on the definition of time of concentration as time between the end of rainfall and the inflection point of the falling limb of the hydrograph (figure 4).

These two methods give different values for the time of concentration. These results parallel the different values for time of concentration found in the experimental work, depending on whether the water was introduced by the rainfall simulator or through flood irrigation. The fact that each exploration determined different times of concentration depending on the system or time definition points out an important inconsistency in practice: how is the time of concentration defined?
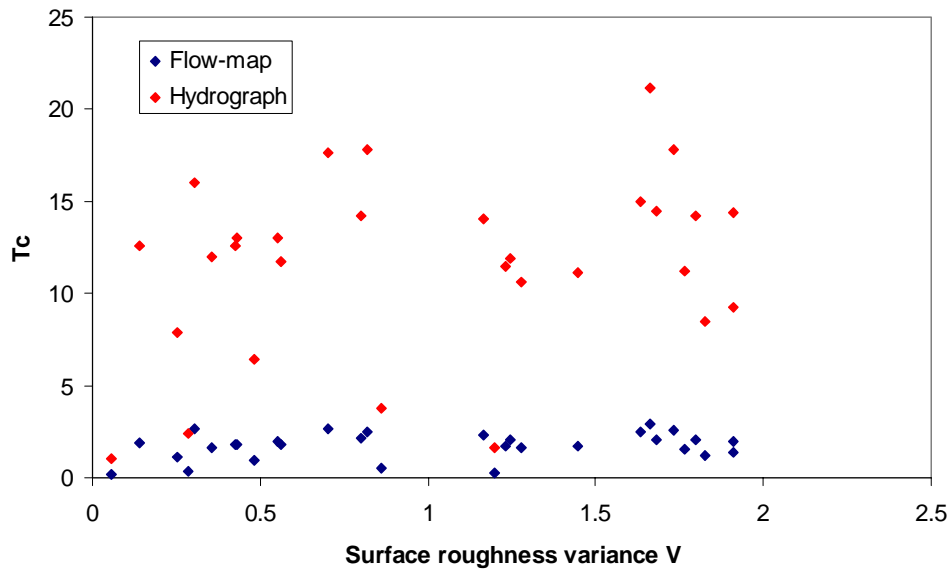
Figure 4. Time of Concentration as a Function of Surface Roughness Variance.

Results from 30 acceptable simulation runs are presented in figures 5 through 7. Time of concentration defined by each method is shown as a function of overall (large-scale) slope, surface roughness variance, and Manning's n. Times of concentration determined by means of the hydrograph based method are considerably longer than those determined by the flow path method. There is, however, no clear functional relationship between either of the types of times of concentration and the supposed explanatory variables.
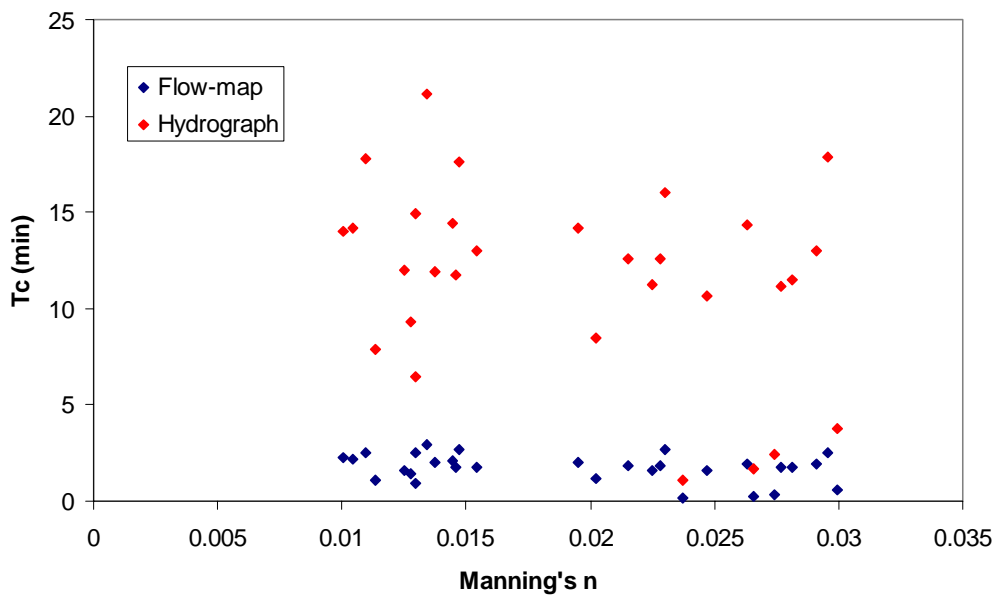
Figure 5. Time of Concentration as a Function of Surface Type. (parameterized by a random Manning's n).
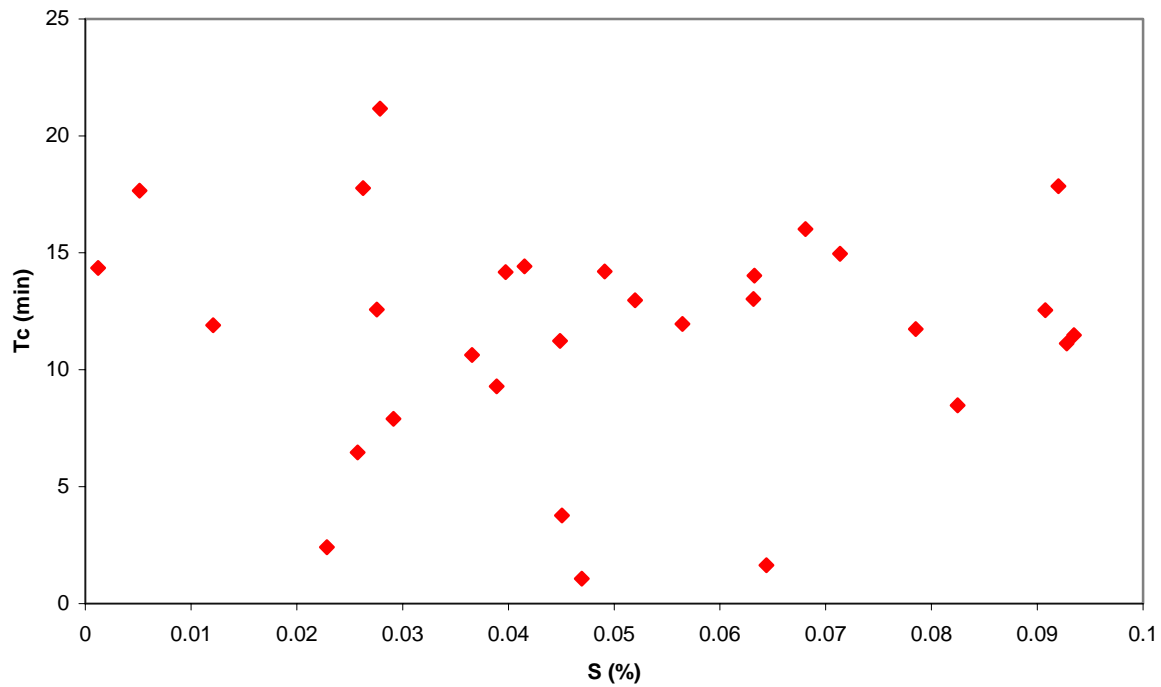
Figure 6. Time of Concentration as a Function of Large-Scale Slope (A).
(Time of concentration is determined from the hydrograph.)
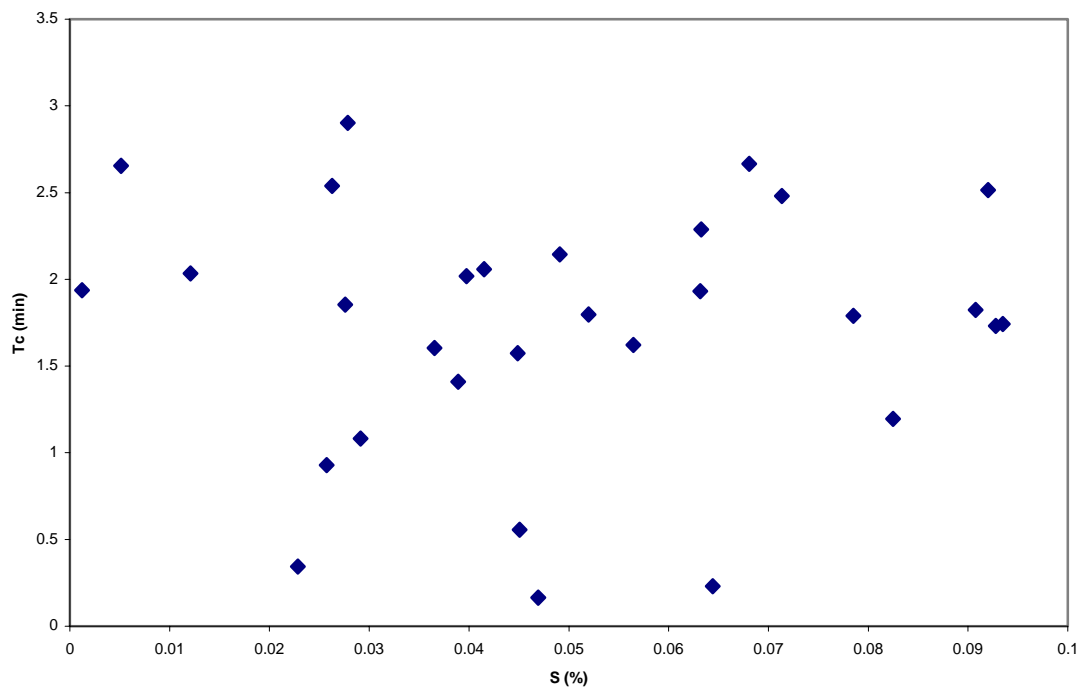
Figure 7. Time of Concentration as a Function of Large-Scale Slope (B).
(Time of concentration is determined from the flow-map.)

Researchers conclude that the absence of the expected correlation between the time of concentration calculated by the model and the variables of interest (slope, roughness) is due to:

- shortcomings in the numerical model, especially the treatment of the bottom boundary layer, and
- the lack of correlation in the roughness elements that may be present in real surfaces.

NUMERICAL EXPERIMENT CONCLUSIONS

Based on the results of the successful numerical simulations, we found that for regions with extremely low overall slope, random microtopography highly influenced the flow rate. Certain "lucky" surfaces had relatively high flow rates because of good interconnectedness. "Unlucky" surfaces had more surface detention and corresponding lower flow rates. Until we are better able to characterize surface roughness properties in this sort of model, consideration of microtopography will lead to this sort of result.

Numerical stability was a real problem in this type of simulation. Alternate methods for treatment of the partial differential equations that describe the flow may yield better results, but at a cost of greater computational complexity. The lack of a large number of simulations had on the determination of the functional relationship between time of concentration and the variables of interest.

CHAPTER 2:
LABORATORY EXPERIMENT

INTRODUCTION

Researchers conducted the laboratory experiment to provide data for validation. By comparing the numerical modeling results with the laboratory experiment results, the numerical model could be adjusted to improve the runoff travel time prediction. Two types of experiments were conducted: rainfall test and impulse runoff test on all test plots.

RAINFALL TEST

The rainfall test used a mobile artificial rainfall simulator (figure 8) on prepared flat surfaces. The simulator included a hydroseeder with a 500-gallon water tank and an 18-inch-high rain rack with spray nozzles mounted in a 5-foot spacing. This rainfall simulator was designed to cover the entire test plot. The hydroseeder pump generated a flow ranging from approximately 15 to 41 GPM. At this flow rate, the precipitation rate generated by the spray nozzles ranged from 1.5 to 3.3 in/hr.

Each test plot measured 6 feet wide by 30 feet long. This size allowed each rainfall test to run for more than 45 minutes using the maximum capacity 500-gallon water tank. A 45-minute rainfall could almost guarantee the test would reach the time of concentration.

Test Procedure

Each rainfall test followed the procedure outlined below:

- measure the surface soil moisture except on the concrete and asphalt surfaces,
- determine precipitation rate,
- start pump to begin test,
- observe runoff condition at the lower end of the test plot,
- measure runoff rate,

Figure 8. Artificial Rainfall Simulator.

- turn off hydroseeder pump after the runoff peaks for approximately 10 minutes, and

- continue measurement of runoff rate until the runoff ceases.

IMPULSE RUNOFF TEST

The impulse runoff test evaluated the runoff travel time. As with the rainfall test, researchers used a hydroseeder as the mobile water source. A large reservoir held water injected from the hydroseeder. This reservoir, during an impulse runoff test, was placed on the higher end of the test plot to allow water to overflow its weir (figure 9). The hydroseeder pump generated a flow ranging from approximately 15 to 41 GPM. The size of each test plot measured 6 feet wide by 30 feet long, the same as the rainfall test.

Figure 9. Resevoir and Hydroseeder.

Test Procedure

Each impulse runoff test followed the procedure outlined below:

- prior to each test, water pervious test plots, including bare clay, lawn, and pasture to create a saturated condition;

- determine runoff rate;

- start pump to begin the test;

- measure travel time after water overtopped the weir; and

- continue travel time measurements until the waterfront reaches the outlet.

TESTED SURFACES AND NUMBER OF TESTS

Surface types tested in this research included:

- **Bare clay**. Two plots were bare clay. The soil texture for the clay tested in this research was 21 percent sand, 31 percent silt, and 48 percent clay. The slope of these two bare clay plots was 0.43 percent.

- **Lawn**. Two plots were lawn. The lawn was formed using Bermuda grass. Lawn condition was maintained by mowing. The slopes of these two lawn plots were 0.48 percent and 0.24 percent, respectively.

- **Pasture**. Two plots were pasture. Pasture was defined as 6 inches or taller grasses. The slopes of these two pasture plots were 0.48 percent and 0.24 percent, respectively.

- **Concrete**. One plot was concrete. The slope of this plot was 0.35 percent.

- **Asphalt**. One plot was asphalt. The slope of this plot was 0.35 percent.

The test number on different test surfaces is presented in table 1.

Table 1. Number of Tests.

Tested surfaces	Rainfall test	Impulse runoff test
Bare clay	11	15
Lawn	13	N/A
Pasture	12	14
Concrete	10	1
Asphalt	7	16

The data and the range of that specific data category collected in this research are summarized in the following list:

- Slope: 0.24 – 0.48 percent
- Rainfall intensity (for rainfall tests): 1.5 – 3.3 in/hr
- Runoff flow rate (for impulse runoff tests): 15 – 41 GPM
- Antecedent soil moisture (on bare clay, lawn and pasture): 8 – 54%
- Infiltration rate: 0.0358 – 0.0598 in/hr
- Soil texture: 21 percent sand, 31 percent silt, and 48 percent clay
- Raindrop size: 0 – 0.07 inch in diameter
- Time to peak (rainfall test) or travel time (impulse runoff test)

RESULTS AND DISCUSSION

Rainfall Test

A typical hydrograph of the rainfall test is shown in figure 10. Depending on the antecedent moisture, rainfall intensity, and surface type, the time to peak and time of beginning of runoff varied. All hydrographs of the rainfall test are presented in the Appendix.
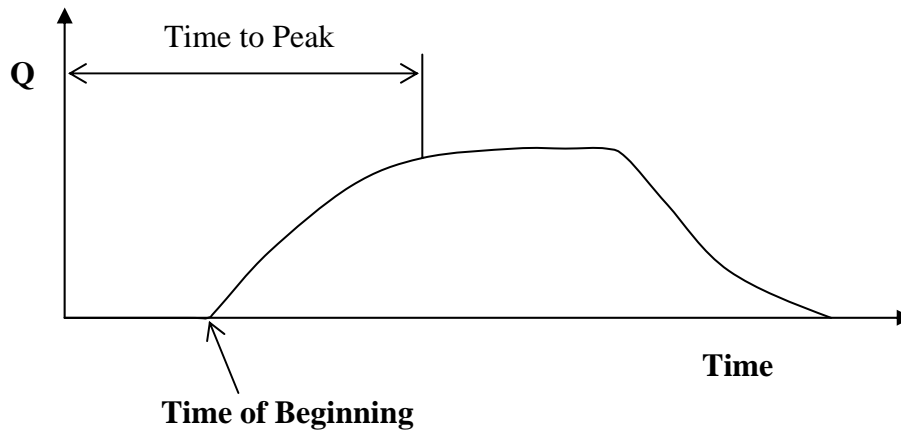
Figure 10. Typical Hydrograph in a Rainfall Test.

Comparisons of the measured time and other variables were conducted. Figure 11 shows the relationship between the time to peak and the antecedent moisture content on pervious surfaces (bare clay, lawn, and pasture).
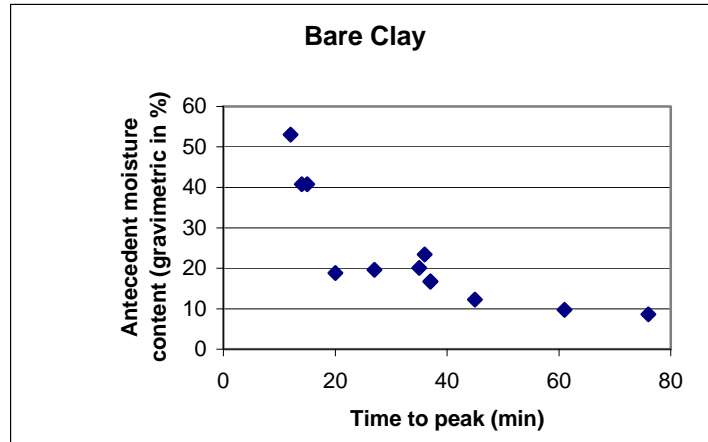
(a)
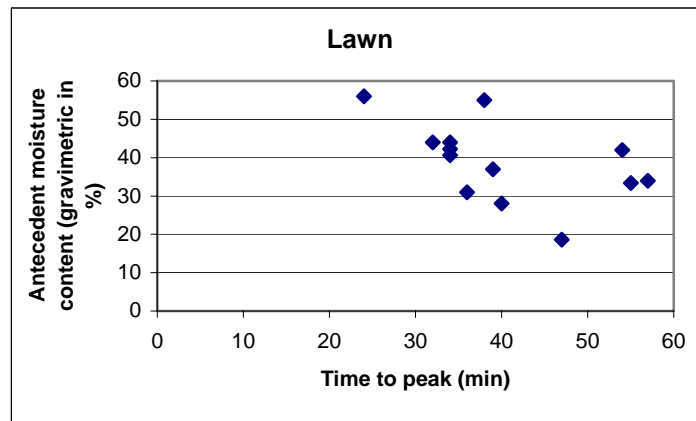
(b)
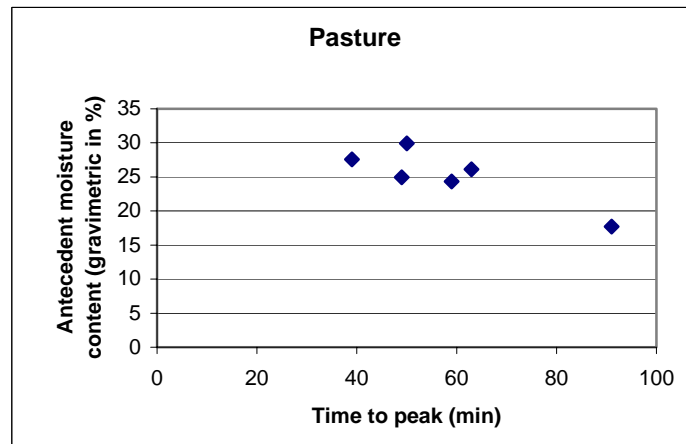
(c)

Figure 11. The Relationship of Time to Peak and Antecedent Moisture Content on Rainfall Tests. (a) Bare Clay, (b) Lawn, and (c) Pasture.

It appears that the higher the antecedent moisture, the shorter the time to peak runoff flow rate.

Similarly, the reversely proportional relationships between the time of beginning and antecedent moisture as well as that between the time to peak and the rainfall intensity were also observed. These relationships are plotted in figures 12 and 13.
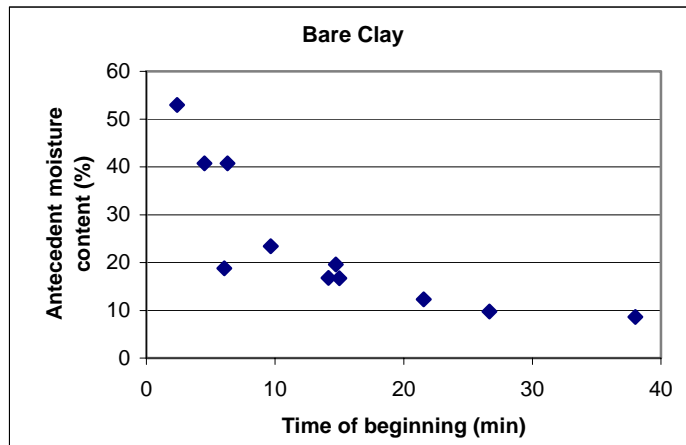
(a)
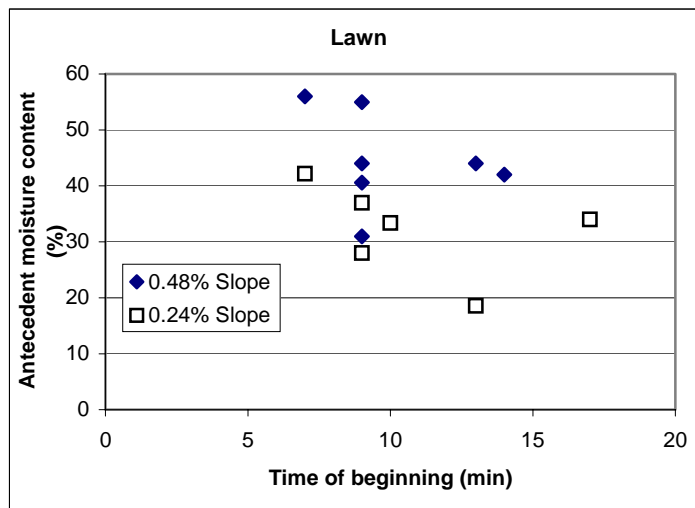
(b)
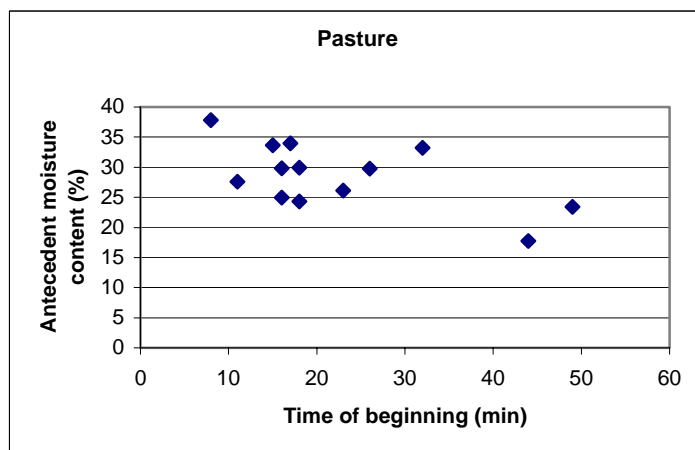
(c)

Figure 12. The Relationship of Time of Beginning and Antecedent Moisture Content on Rainfall Tests. (a) Bare Clay, (b) Lawn, and (c) Pasture.

21
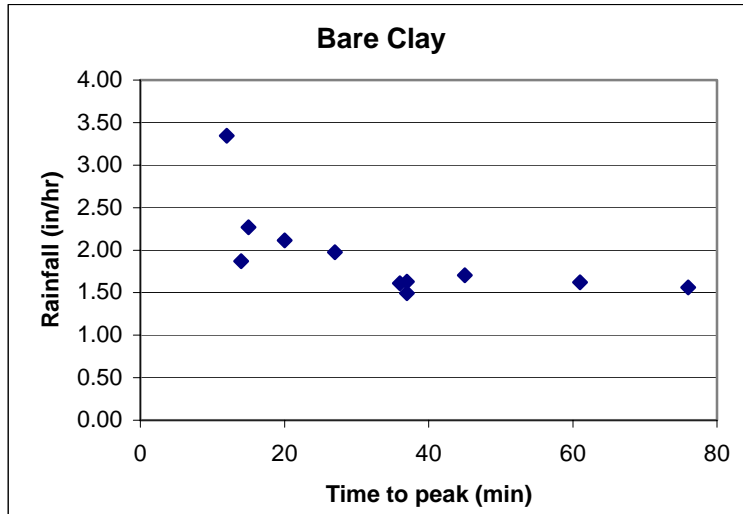
(a)
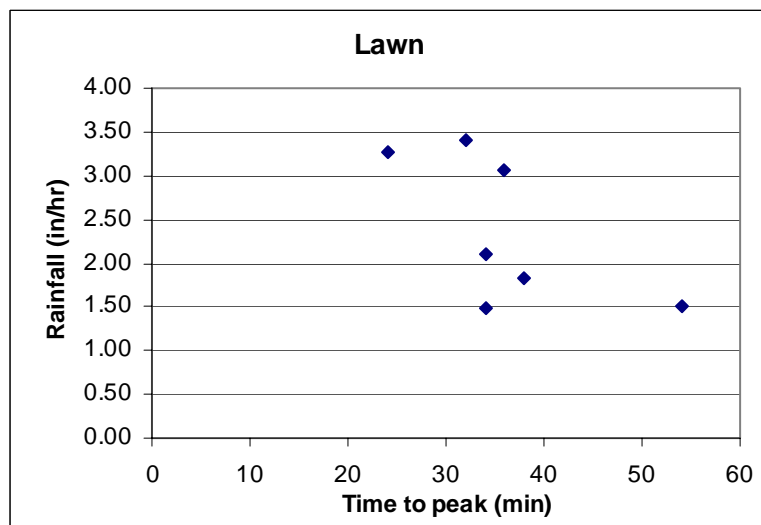
(b)

Figure 13. The Relationship of Time to Peak and Rainfall Intensity on Rainfall Tests. (a) Bare clay, (b) Lawn
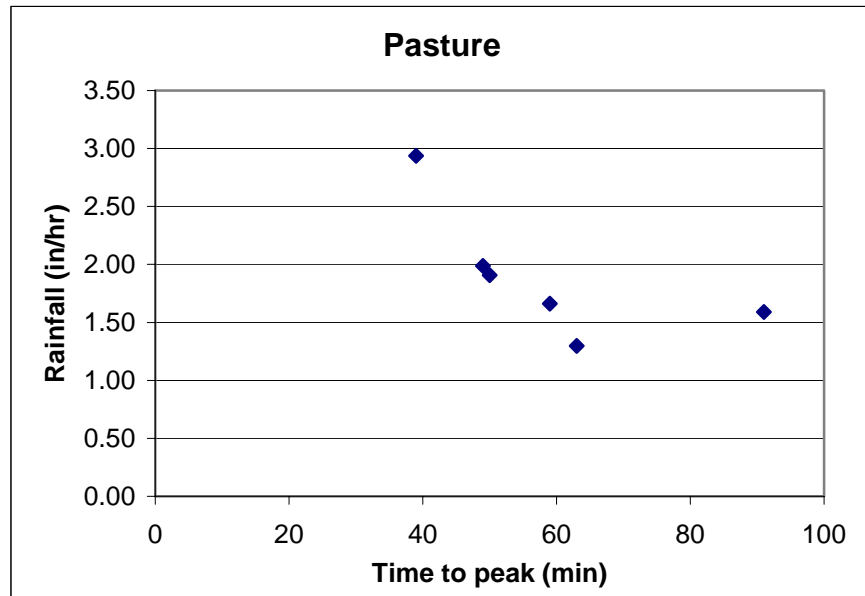
(c)
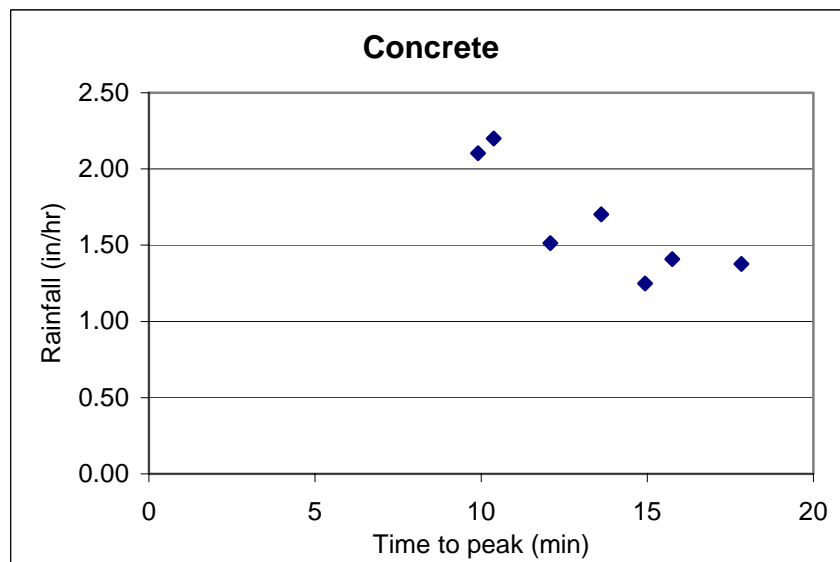
(d)

Figure 13 (cont.). The Relationship of Time to Peak and Rainfall Intensity on Rainfall Tests.   (c) Pasture and (d) Concrete.

The linear regression analysis of the laboratory data was further conducted to create a model that may predict runoff travel times. The most comprehensive model to predict the time of concentration summarized from more than 10 models by Papadakis and Kazan (1986) included four independent variables:

- length of the watershed,
- surface roughness (usually Manning's n),
- slope of the watershed, and
- rainfall intensity.

The model is expressed as:

$$T_c = kL^a n^b S^{-y} i^{-z} \tag{1}$$

where T_c is the time of concentration, L is the watershed length, n is Manning's n, S is the watershed slope, and i is the rainfall intensity. k is a constant and a, b, y, z are exponents. This equation exhibits a linear correlation of the logarithms of the variables involved.

Researchers found that the antecedent soil moisture appeared to influence the runoff travel time. Using the above model as the baseline model researchers added the antecedent soil moisture variable to create a new model. It is expressed as:

$$T_c = kL^a n^b \theta^{-x} S^{-y} i^{-z} \tag{2}$$

where the added variable θ is the antecedent soil moisture, and x is an exponent of θ. For the new model, the watershed length (L) is 30 feet, which is the length of all test plots, and the exponent of 0.5 used for L is the mean of several models from Papadakis and Kazan (1986). The model developed from the laboratory data is:

$$T_c = 0.951 \cdot L^{0.5} n^{0.326} \theta^{-0.459} S^{-0.053} i^{-0.674} ; (L = 30 \text{ ft}) \tag{3}$$

where T_c is the time of concentration in minutes, L is the watershed length in feet, n is Manning's n, θ is the antecedent soil moisture in percent, S is the watershed slope, and i is the rainfall intensity in in/hr. The *p-values* of each independent variable are presented in Table 2. It appears that S variable has the least influence on the time of concentration because the exponent for S is the least among all variables. This could result from fewer slopes tested in the research (0.24 percent, 0.35 percent, 0.43 percent and 0.48 percent). Or, if slope data number is not the cause, the least effect from S might conclude that when slope is very flat, the effect from variables θ, n, and i are dominant on the time of concentration.

Table 2. Predicting Variables (*p-values*) in the New Runoff Travel Time Model.

	Coefficients	*p*-value
k (constant)	0.951141	0.002271
x (exponent of θ)	-0.45881	3.58E-12
b (exponent of n)	0.32583	2.99E-17
y (exponent of S)	-0.05261	0.643592
z (exponent of i)	-0.67431	2.92E-06

Overall, the developed model appears to predict the observed time of concentration well (see figure 14).
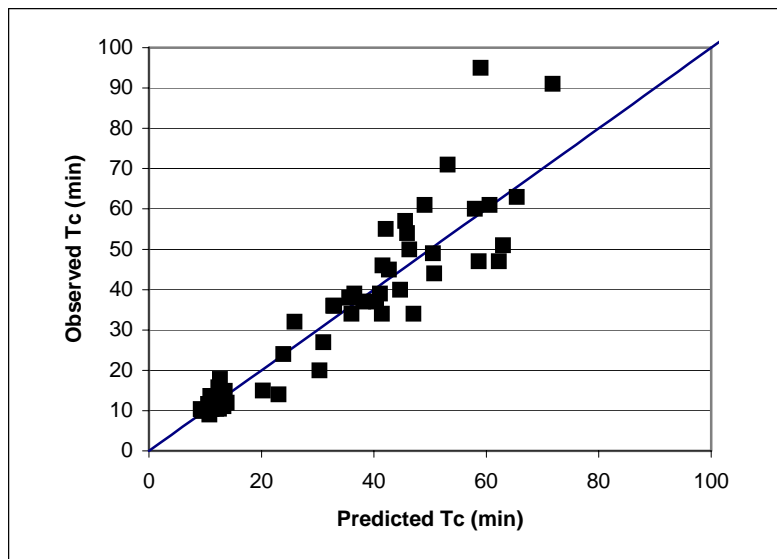
Figure 14. Observed vs. Predicted Time of Concentration in the Rainfall Test.

To investigate how other models predict the observed result in this research, the Papadakis and Kazan (1986) and Izzard models were compared with the new developed model (equation 3). Papadakis and Kazan's (1986) is expressed as:

$$T_c = 0.6L^{0.5}n^{0.52}S^{-0.31}i^{-0.38} \qquad (4)$$

Izzard model is expressed as:

$$T_t = \frac{41bL^{0.33}}{i^{0.67}} \qquad (5)$$

$$b = \frac{0.0007i + C_r}{S^{0.333}} \qquad (6)$$

where T_t is the travel time in minutes, L is the flow path length in feet, i is the rainfall intensity for duration T_t in inches per hour, and C_r is the roughness coefficient. As plotted in figure 15, both the Papadakis and Karan (1986) and Izzard models underestimate the observed time of concentration. This indicates that it may be inappropriate to use current models to predict time of concentration in very flat areas.
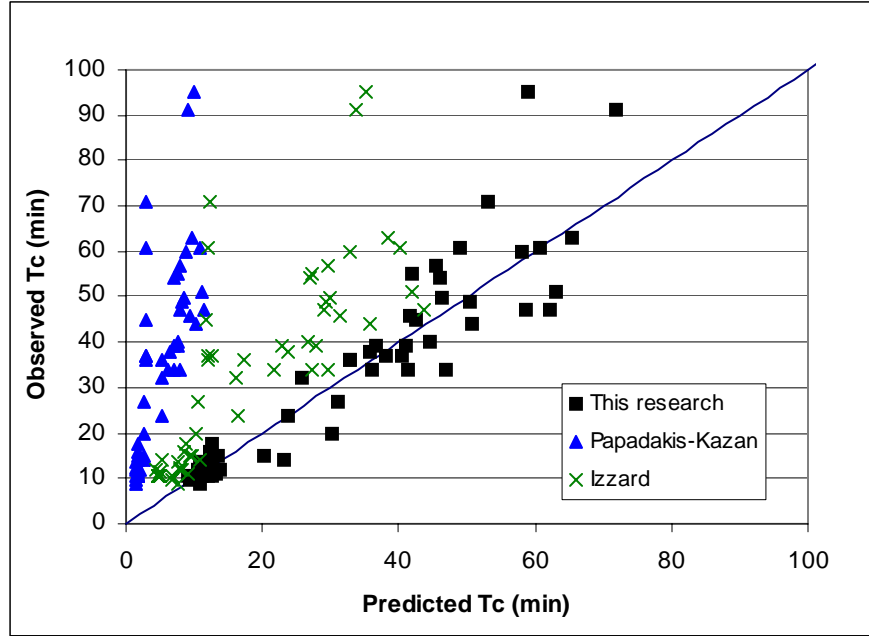
Figure 15. Comparison of Predicted Time of Concentration (three models).

Impulse Runoff Test

In the impulse runoff test, pervious plots including bare clay, lawn, and pasture were watered to create a saturated condition in the top few inches of the surface prior to the test. Impulse runoff was then injected to the test plot from a reservoir for the travel time measurement. Similarly, researchers applied the linear regression analysis to the impulse runoff data and found that the following model predicts the observed data well.

$$T_t = 0.779 \cdot L^{0.5} n^{0.453} Q^{-0.537} S^{-0.037} \tag{7}$$

where T_t is the travel time in minutes, L is the watershed length in feet (30 feet in this research), n is Manning's n, Q is the flow rate in GPM, and S is the watershed slope in percent. Figure 16 shows the observed and the predicted data using Equation (7).
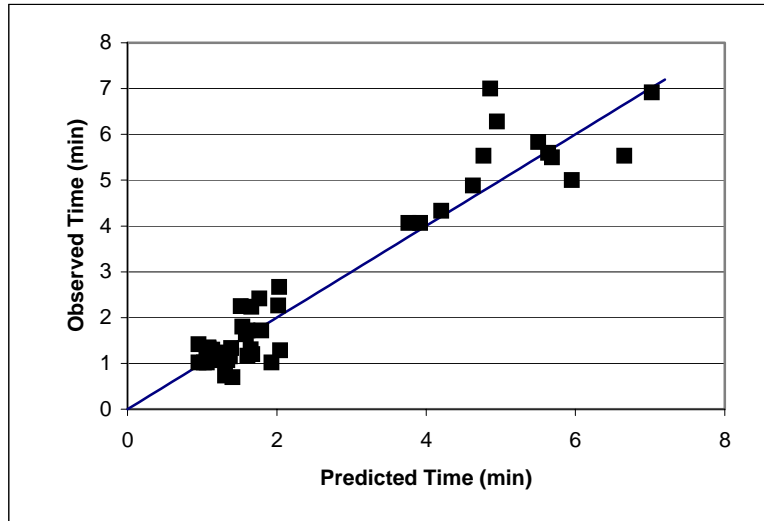
Figure 16. Observed vs. Predicted Travel Time in the Impulse Runoff Test (A).

Researchers also compared current travel time models. TxDOT (1997) and Kirpich (1940) were used in this task, and the comparison plot is presented in figure 17. The Kirpich (1940) model underestimates observed data, whereas TxDOT (1997) overestimates them. Obviously, current models do not accurately predict the runoff travel time in these test conditions.
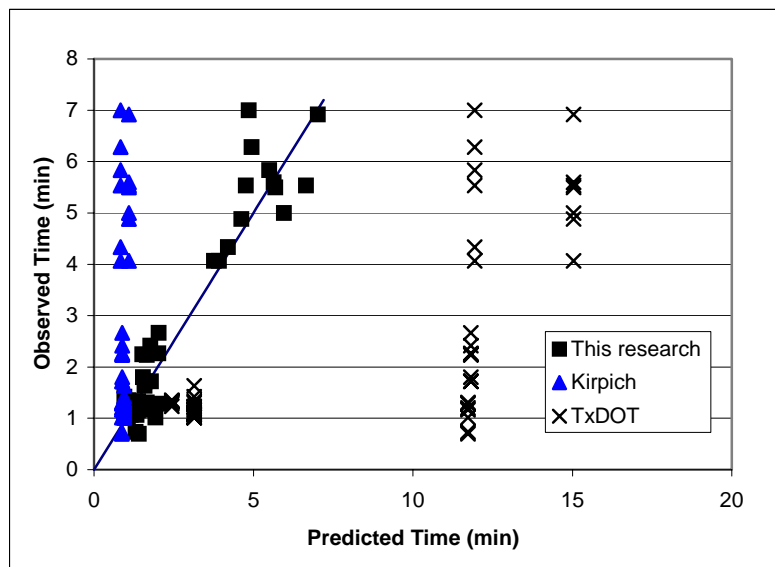
Figure 17. Observed vs. Predicted Travel Time in the Impulse Runoff Test (B).

LIMITATIONS

The limitations associated with the laboratory experiment are summarized in the following list:

- Although the laboratory result is generated under a well-controlled condition, it has not been compared with any flat watershed studies. Without field case studies, laboratory results cannot be scaled up to predict the travel time with confidence.

- In the rainfall test, spray nozzles that generate fine droplets were used to produce simulation rains. Loss of water through evaporation, minor leaks, or breezes was unavoidable.

- There were only a few flat slopes tested in this research.

- Although researchers found that antecedent soil moisture has a significant effect on the time of concentration, they did not monitor changes of soil moisture.

0

RECOMMENDATIONS FOR FUTURE WORK

The findings for this project indicate that the best direction for future work would be through field-scale instrumentation and observation of a number of watersheds with low slope. The rationale for performing the laboratory and numerical studies was the lack of appropriate data as well as the desire to develop a relationship between time of concentration and the explanatory variables without having to collect several years of data. Although data could ultimately be used for a regression-type relationship once collected, any measurements will be of use, to at least provide guidance for future numerical and laboratory modeling.

These watersheds should be in the size range of interest to TxDOT, relatively undeveloped (to avoid the problems urbanization causes in estimating time of concentration), and with similar cover/soil type across the watershed. Watersheds should of course have an overall slope that is very low, 1 percent or less, since these are the watersheds for which current equations overestimate the time of concentration. An initial characterization of the watershed in terms of surface roughness and cover type is required. Continual measurements of rainfall and watershed outflow are the primary data to be collected. Depending on the size of the watershed, more than one rain gauge may be needed, although it is expected that given the size of interest (~100 ac), one gauge may suffice. The sites should also be located in areas of the state where TxDOT has had problems with time of concentration estimation due to low slopes. Obviously, cost will enter into the decision of how many sites to deploy, but a minimum for eventual valid regression should be 10 sites with differing watershed characteristics (cover and soil type). In light of the realization that antecedent soil moisture may impact on time of concentration, representative soil moisture content data would also be useful. The equipment needed to measure this variable is relatively inexpensive; however, multiple sites would be needed in a watershed, which would complicate the data collection and analysis.

REFERENCES

Akan, A.O. Time of concentration of overland flow, J. Irr. Drain. Eng., 112:283-292, 1986.

Esteves, M.X. Faucher, S. Galle, and M. Vauclin. Overland flow and infiltration modeling for small plots during unsteady rain: numerical results versus observed values, J. Hydrol., 228:265-282, 2000.

Govers, G., I. Takken, and K. Helming. Soil roughness and overland flow, Agronomie, 20:131-146, 2000.

Kirpich, Z.P. Time of concentration of small agricultural watersheds, Civil Engineering, Vol.10, no. 6. 1940.

Lawrence, D.S.L. Macroscale surface roughness and frictional resistance in overland flow, Earth Surf. Process. Landforms, 22:365-382, 1997.

Papadakis, C.N. and M.N. Kazan. Time of concentration in small rural watersheds. Technical Report 101/08/86/CEE, Civil Engineering Department, University of Cincinnati, Cincinnati, Ohio, 1986.

Playan, E., J.M. Faci, and A. Serreta. Modeling microtopography in basin irrigation, J. Irr. Drain. Eng., 122:339-347, 1996.

Rouhipour, H., C.W. Rose, B. Yu, and H. Ghadiri. Roughness coefficients and velocity estimation in well-inundated sheet and rilled overland flow without strongly eroding bed forms, Earth Surf. Process. Landforms, 24:233-245, 1999.

TxDOT.Hydraulic Design Manual. Texas Department of Transportation, Austin, Texas, 1997.

Zhang, W. and T.W. Cundy. Modeling of two-dimensional overland flow, Water Resourc. Res., 25:2019-2035, 1989.

APPENDIX
TEST RESULTS
(RAINFALL AND IMPULSE RUNOFF TESTS)
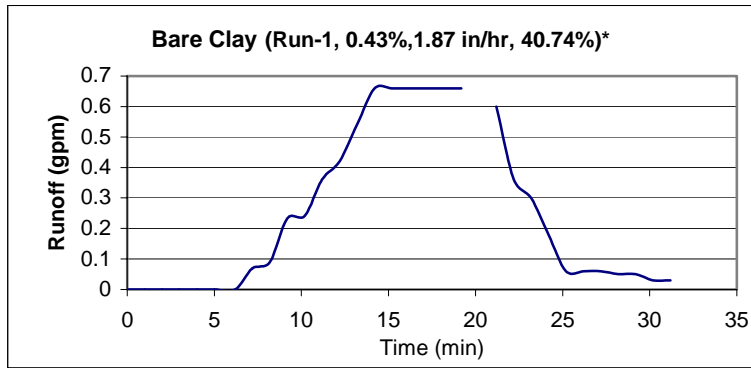
Figure A.1 Rainfall test on bare clay (test 1)

* (test number, surface slope, rainfall intensity, antecedent moisture)
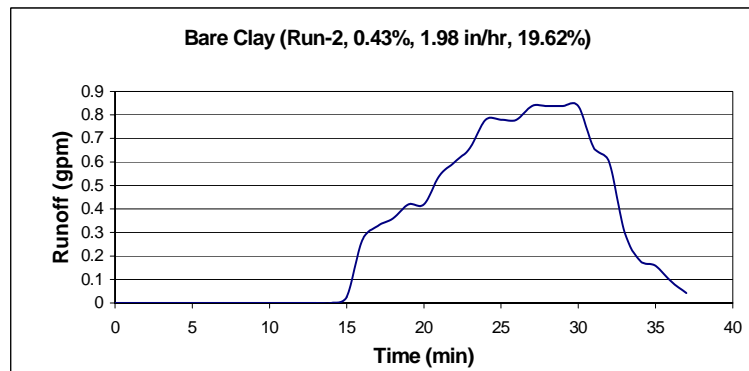
Figure A.2 Rainfall test on bare clay (test 2)
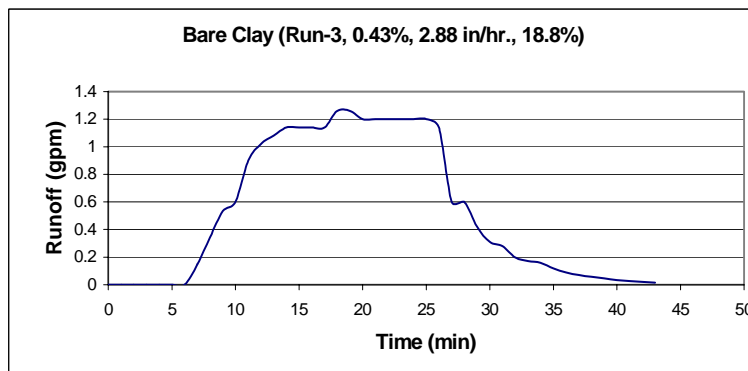
Figure A.3 Rainfall test on bare clay (test 3)
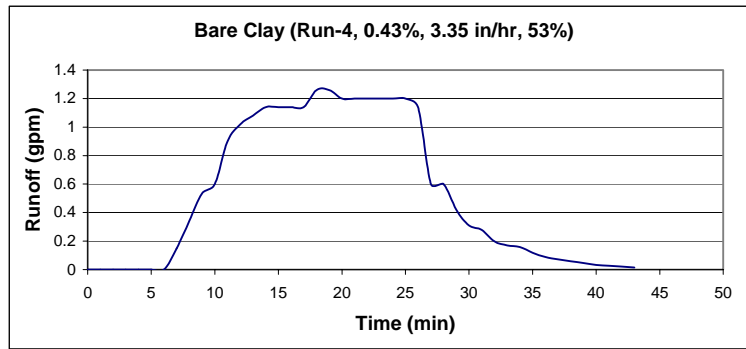
Figure A.4 Rainfall test on bare clay (test 4)
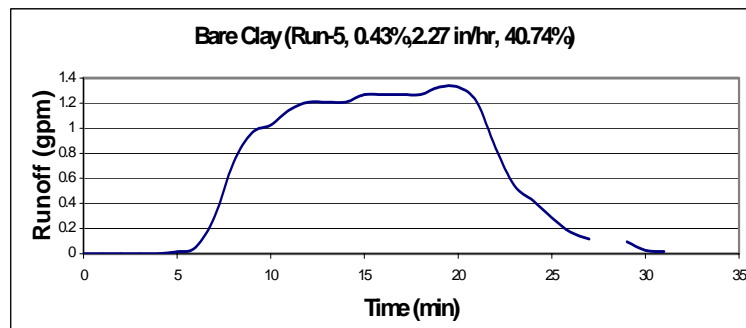
Figure A.5 Rainfall test on bare clay (test 5)
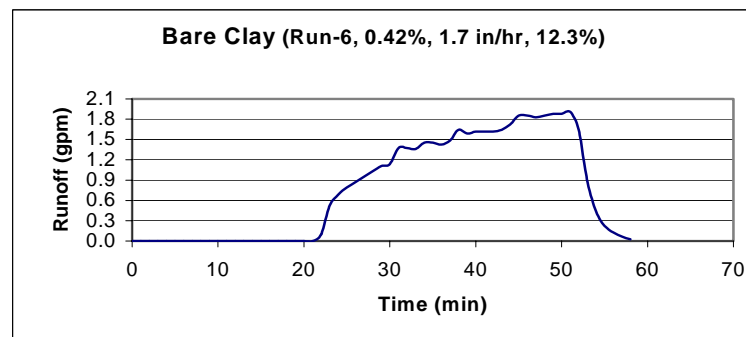
Figure A.6 Rainfall test on bare clay (test 6)
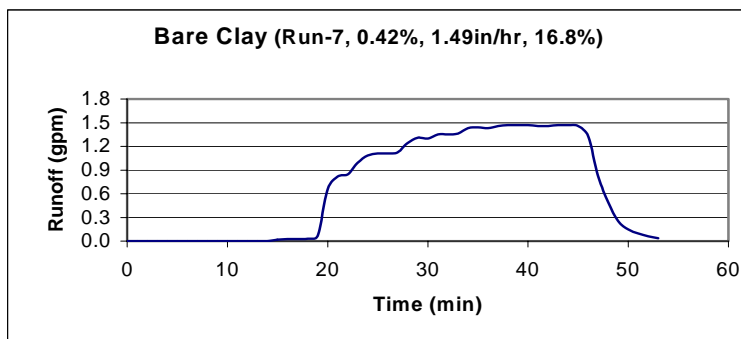
Figure A.7 Rainfall test on bare clay (test 7)
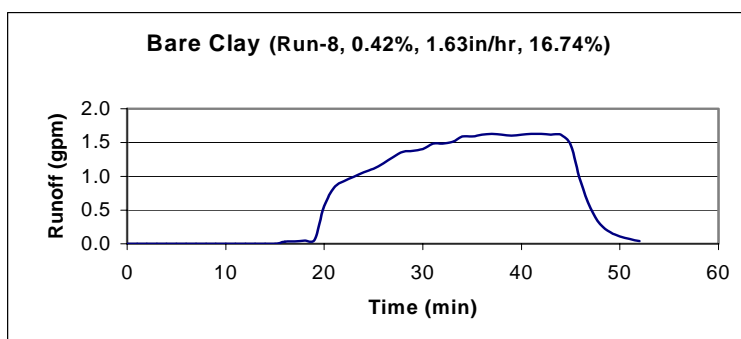
Figure A.8 Rainfall test on bare clay (test 8)
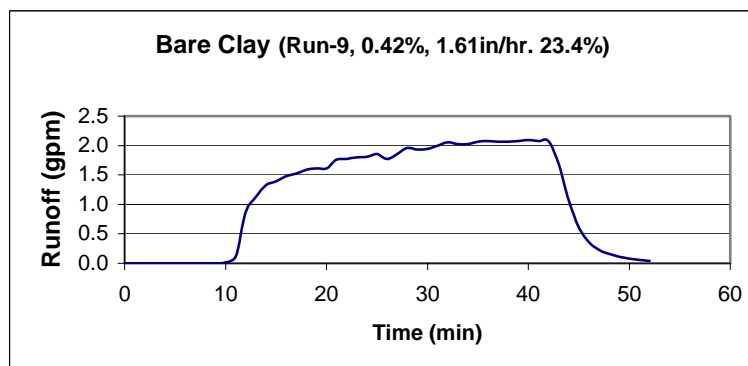
Figure A.9 Rainfall test on bare clay (test 9)
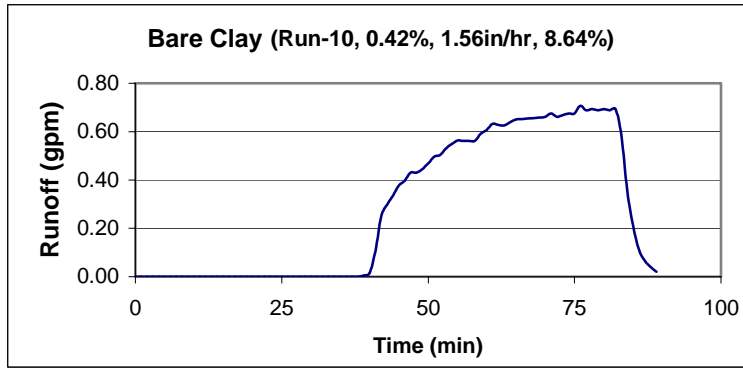
Figure A.10 Rainfall test on bare clay (test 10)
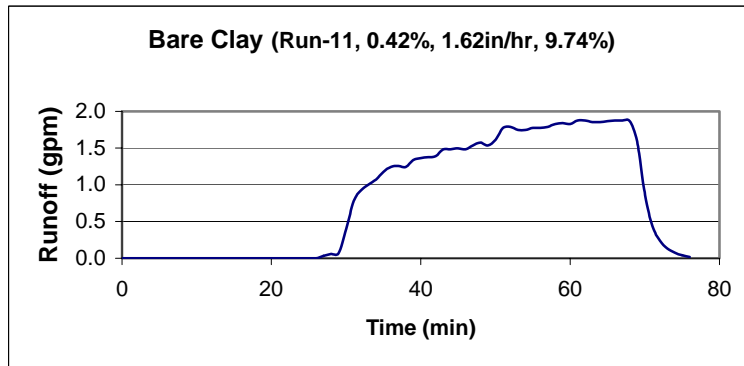
Figure A.11 Rainfall test on bare clay (test 11)
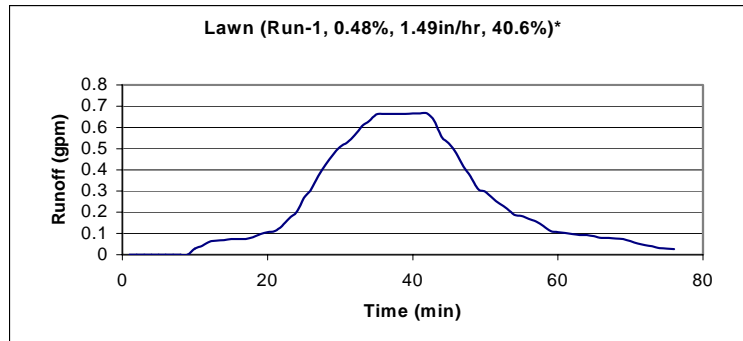
* (test number, surface slope, rainfall intensity, antecedent moisture)

Figure B.1 Rainfall test on lawn (test 1)
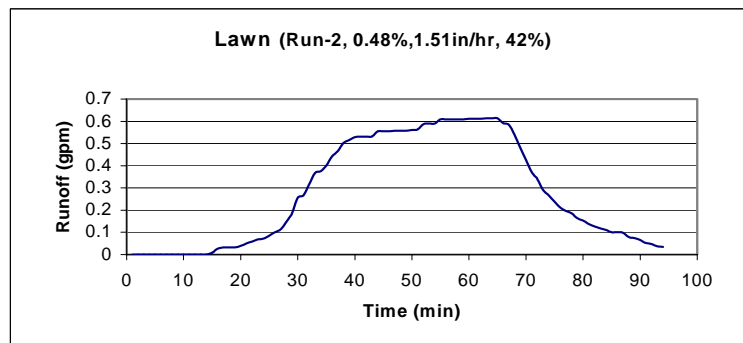
Figure B.2 Rainfall test on lawn (test 2)
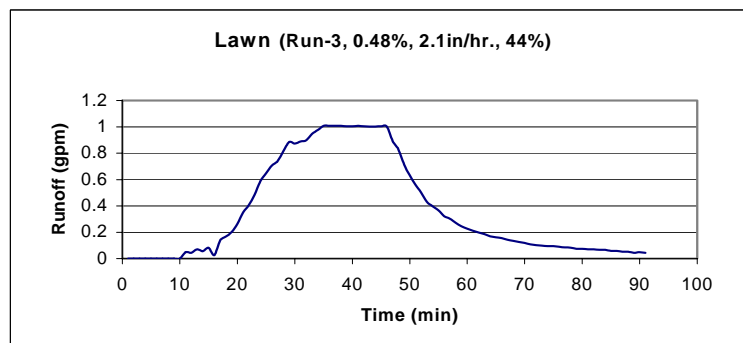
Figure B.3 Rainfall test on lawn (test 3)
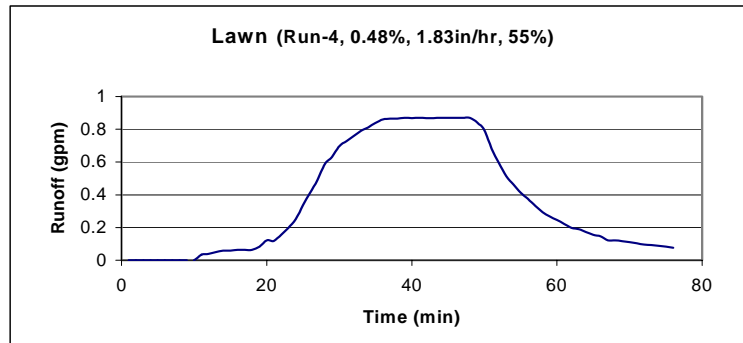
Figure B.4 Rainfall test on lawn (test 4)
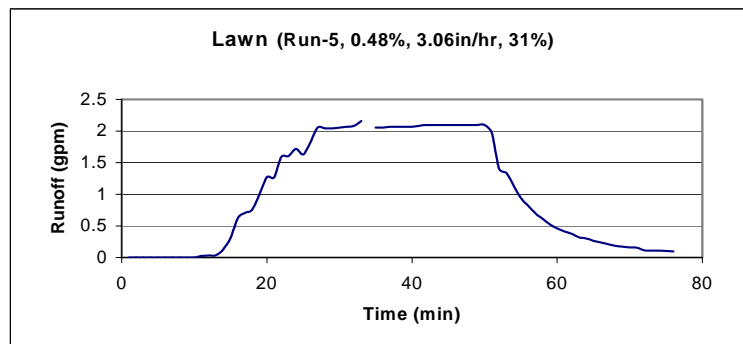
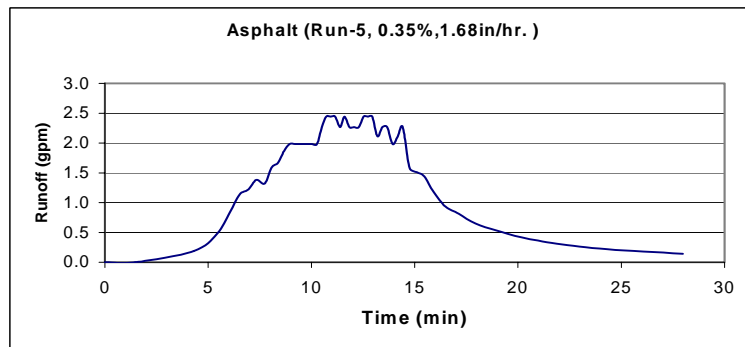

Figure B.5 Rainfall test on lawn (test 5)
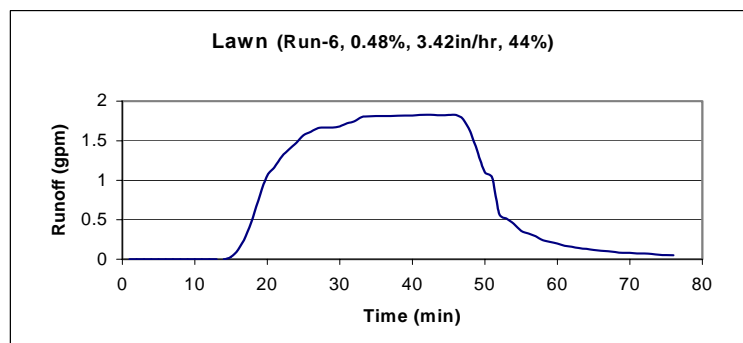
Figure B.6 Rainfall test on lawn (test 6)
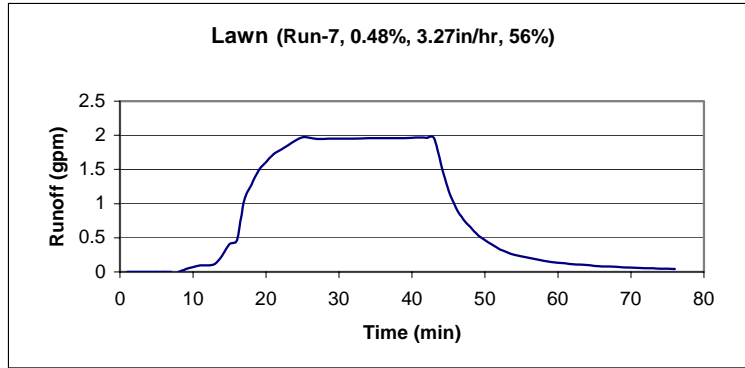
Figure B.7 Rainfall test on lawn (test 7)
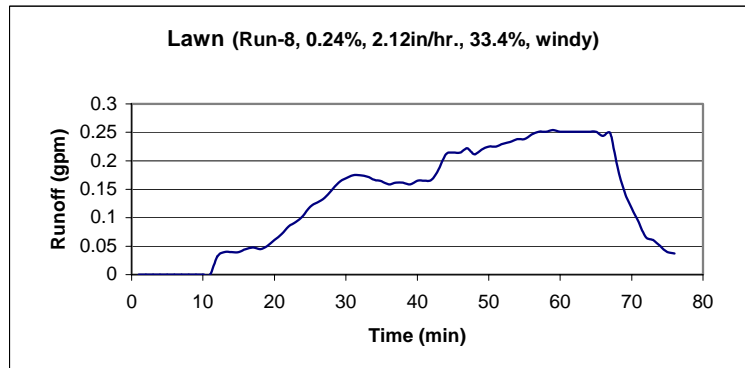
Figure B.8 Rainfall test on lawn (test 8)
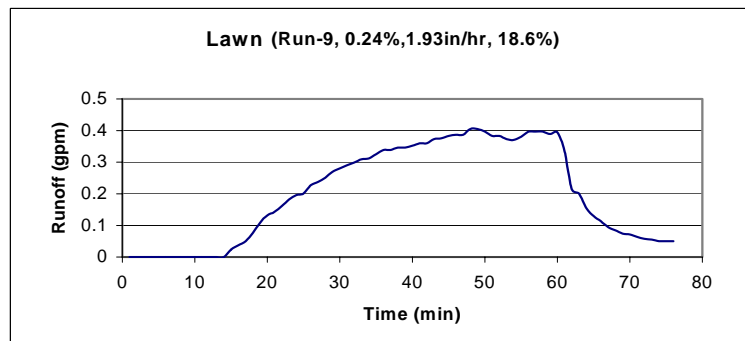
Figure B.9 Rainfall test on lawn (test 9)
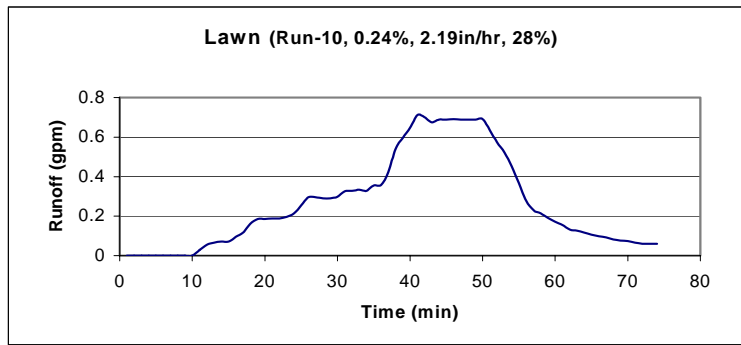
Figure B.10 Rainfall test on lawn (test 10)
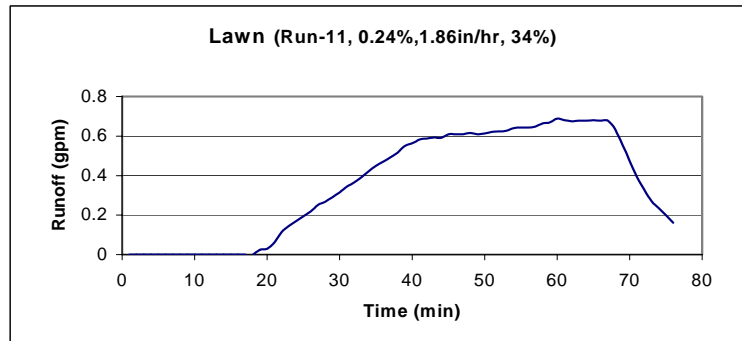
Figure B.11 Rainfall test on lawn (test 11)
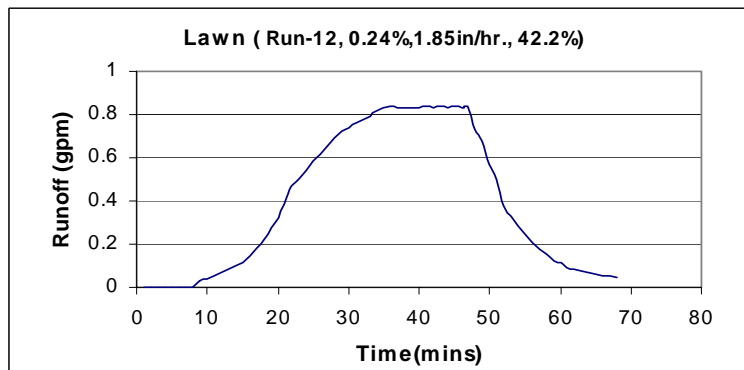
Figure B.12 Rainfall test on lawn (test 12)
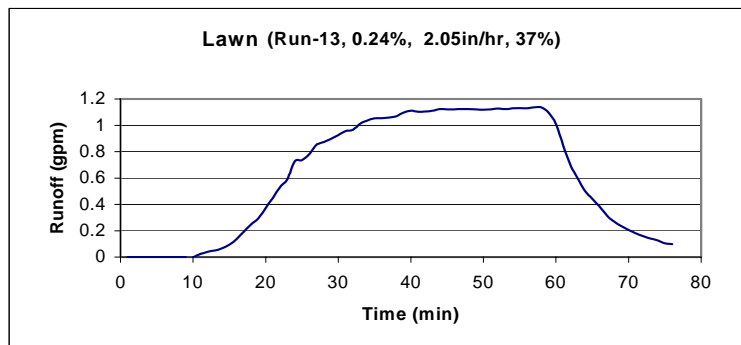
Figure B.13 Rainfall test on lawn (test 13)

Concrete (Run-1, 0.35%, 1.51in/hr.)*
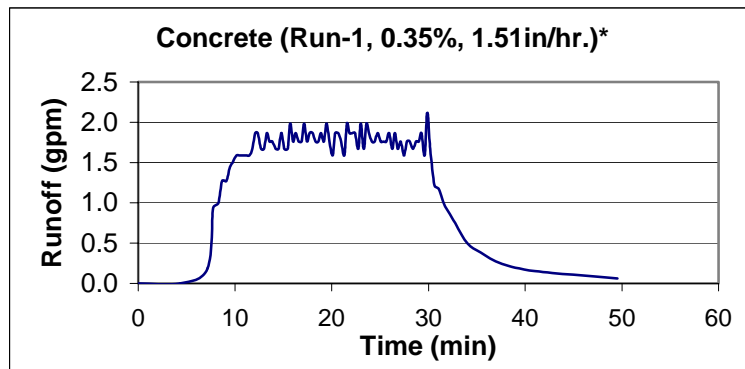
* (test number, surface slope, rainfall intensity)

Figure C.1 Rainfall test on concrete (test 1)

Concrete (Run-2, 0.35%, 1.38in/hr.)
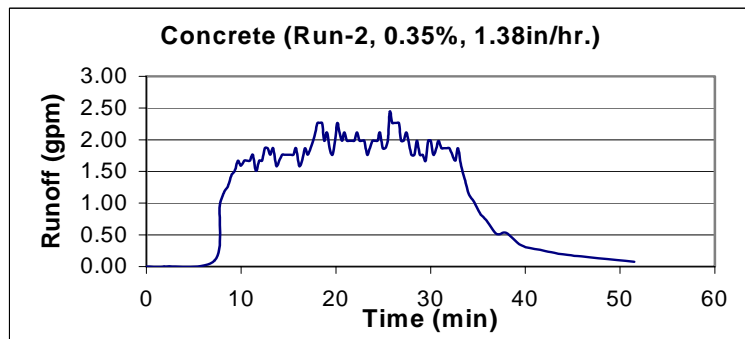
Figure C.2 Rainfall test on concrete (test 2)

Concrete (Run-3, 0.35%, 1.25in/hr.)
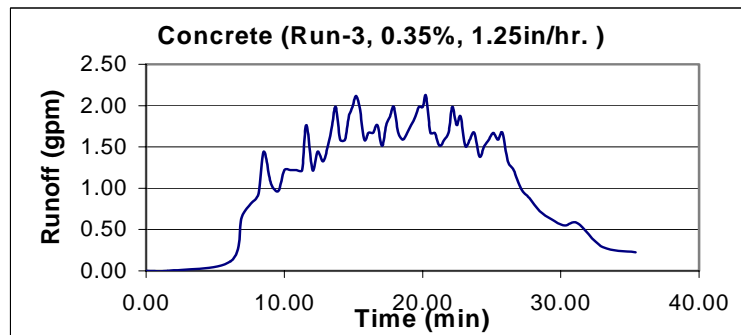
Figure C.3 Rainfall test on concrete (test 3)
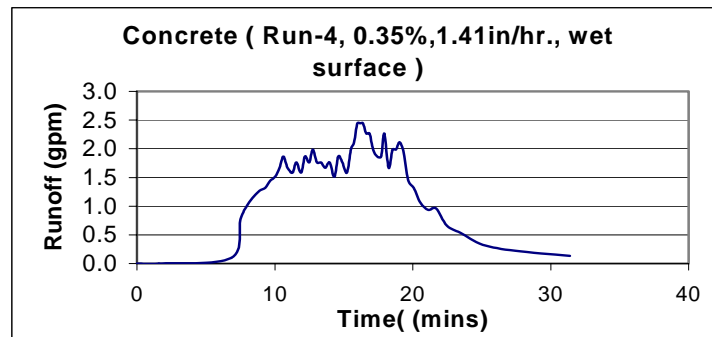
Figure C.4 Rainfall test on concrete (test 4)
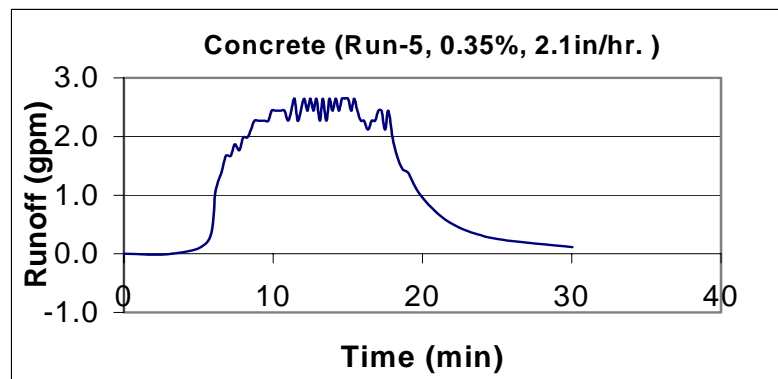
Figure C.5 Rainfall test on concrete (test 5)
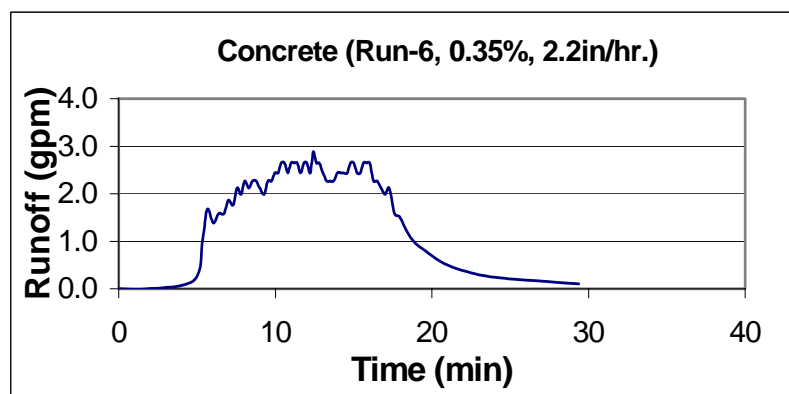
Figure C.6 Rainfall test on concrete (test 6)

Concrete (Run-7, 0.35%,1.70in/hr., wet surface)
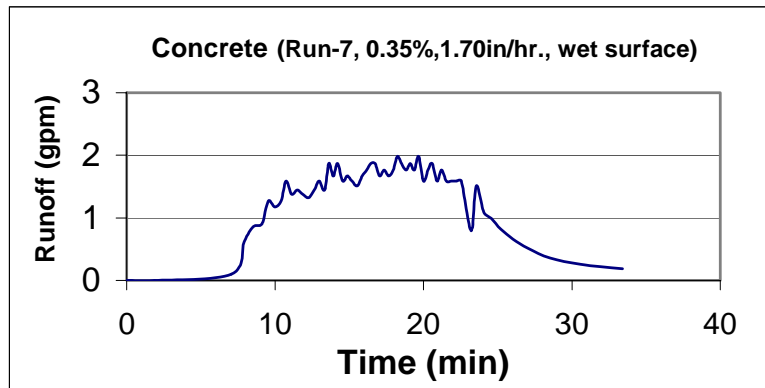
Figure C.7 Rainfall test on concrete (test 7)

Concrete (Run-8, 0.35%,1.62in/hr.)
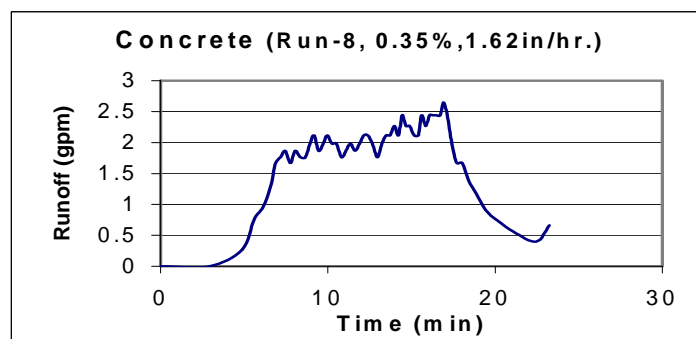
Figure C.8 Rainfall test on concrete (test 8)

Concrete (Run-9, 0.35%,1.74in/hr., wet surface)
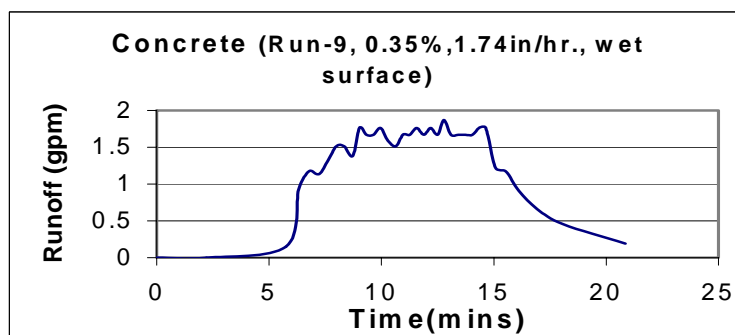
Figure C.9 Rainfall test on concrete (test 9)
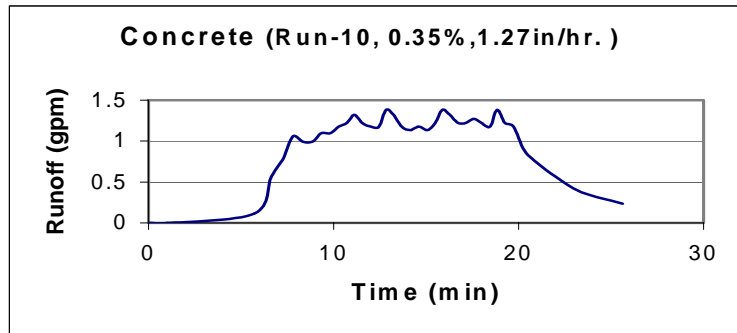
Figure C.10 Rainfall test on concrete (test 10)

Asphalt (Run-1, 0.35%,1.51in/hr.)*
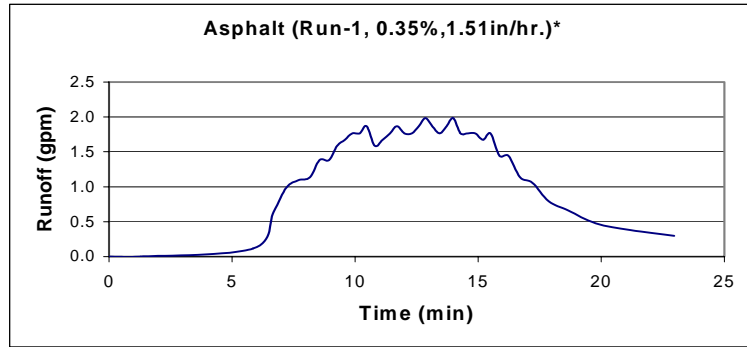
* (test number, surface slope, rainfall intensity)

Figure D.1 Rainfall test on asphalt (test 1)

Asphalt (Run-2, 0.35%,1.6in/hr.,wet surface)
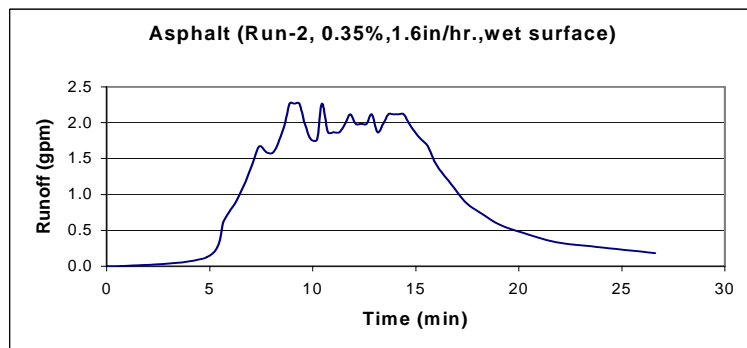
Figure D.2 Rainfall test on asphalt (test 2)

Asphalt (Run-3, 0.35%,1.47in/hr.)
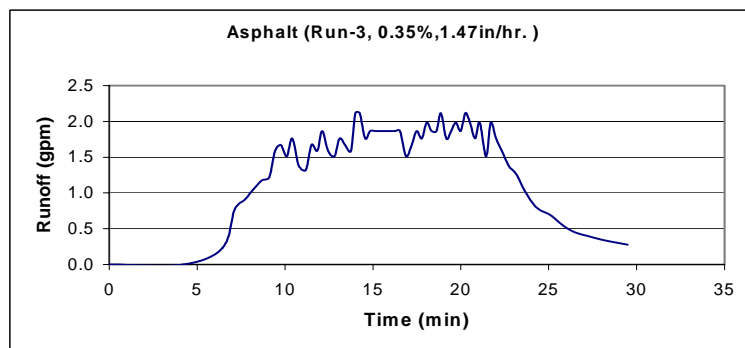
Figure D.3 Rainfall test on asphalt (test 3)
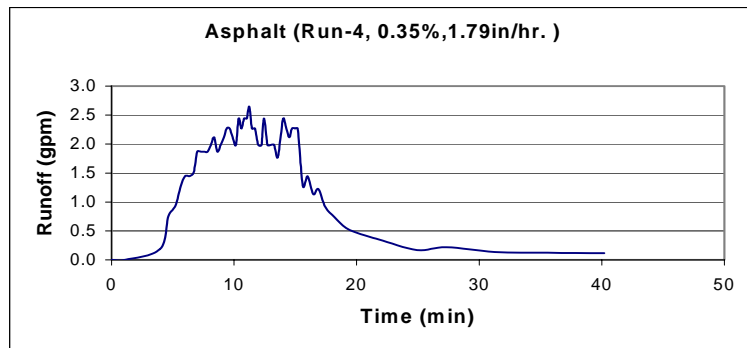
Figure D.4 Rainfall test on asphalt (test 4)

Figure D.5 Rainfall test on asphalt (test 5)
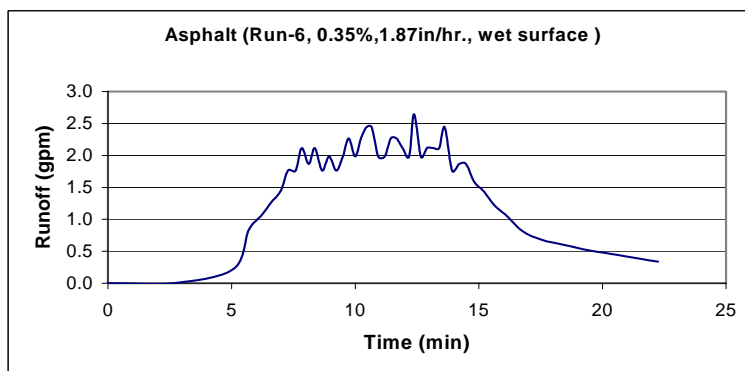
Figure D.6 Rainfall test on asphalt (test 6)

Asphalt (Run-7, 0.35%,1.93in/hr., wet surface)
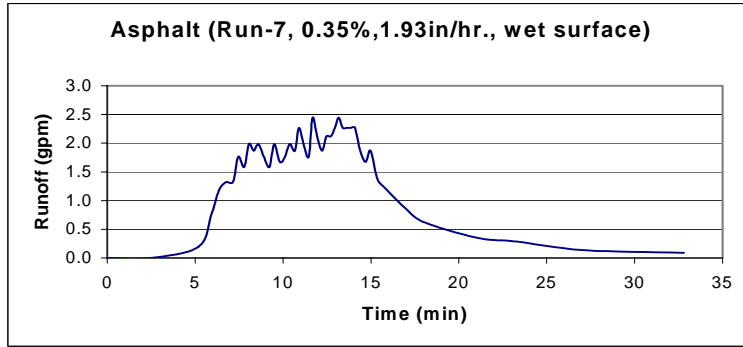
Figure D.7 Rainfall test on asphalt (test 7)
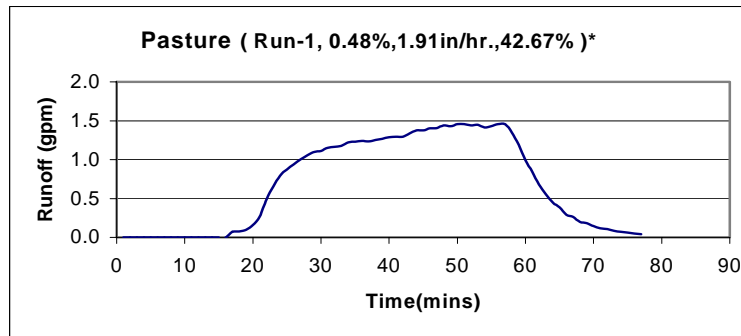
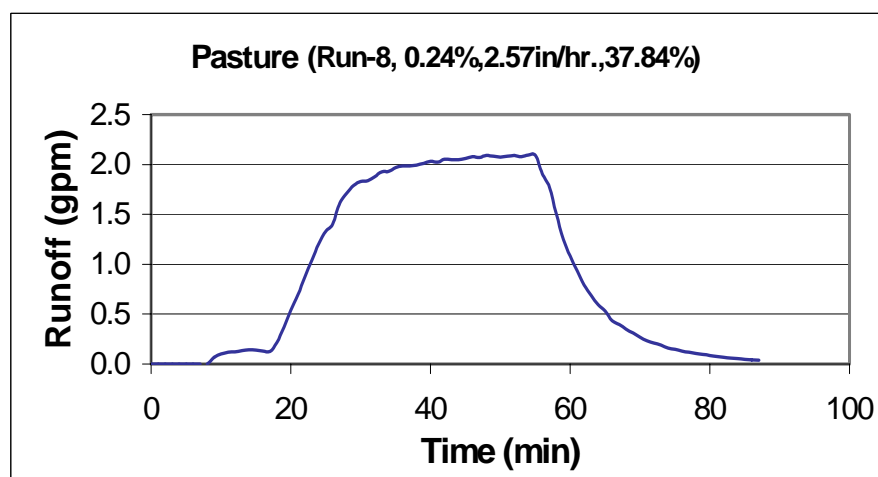* (test number, surface slope, rainfall intensity, antecedent moisture)

Figure E.1 Rainfall test on pasture (test 1)
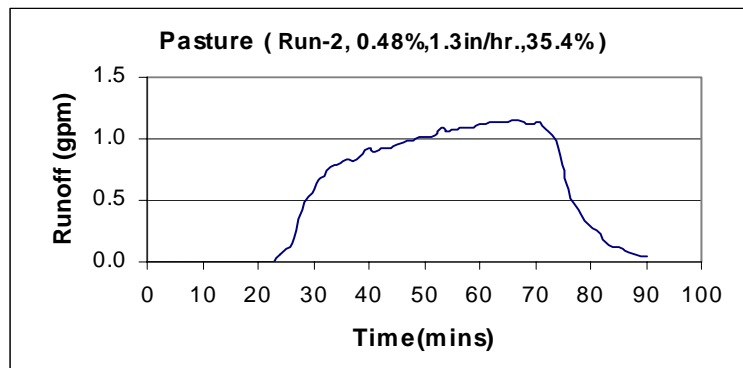
Figure E.2 Rainfall test on pasture (test 2)
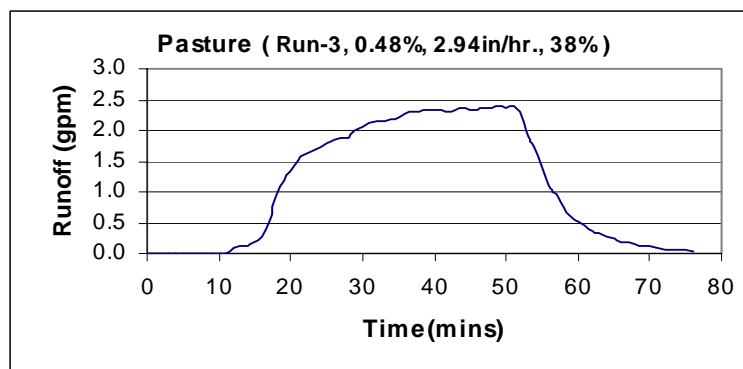
Figure E.3 Rainfall test on pasture (test 3)
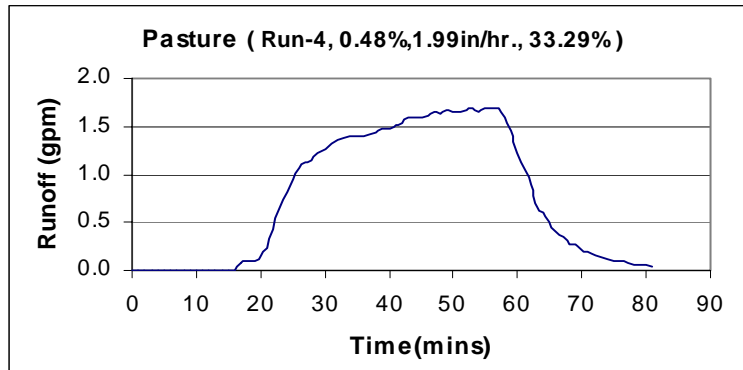
Figure E.4 Rainfall test on pasture (test 4)
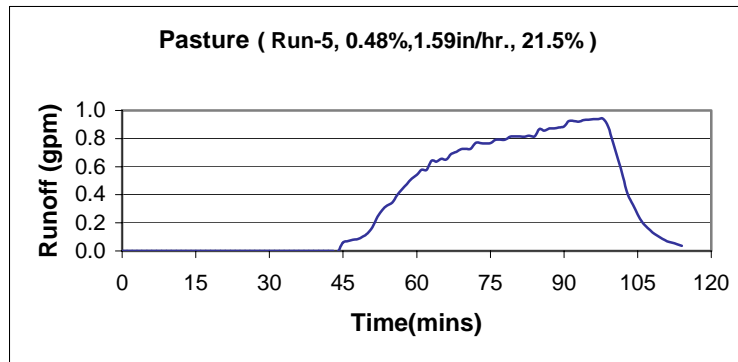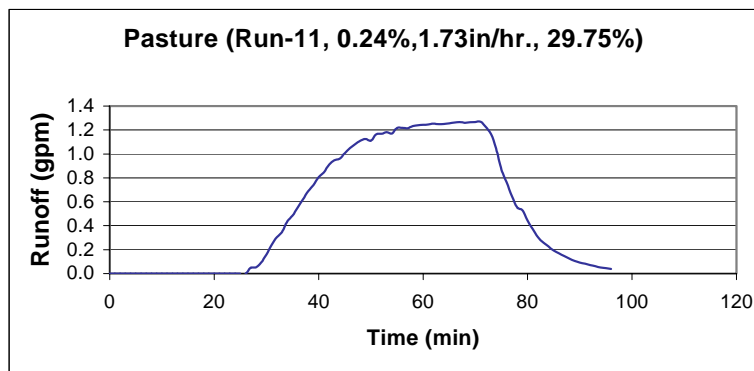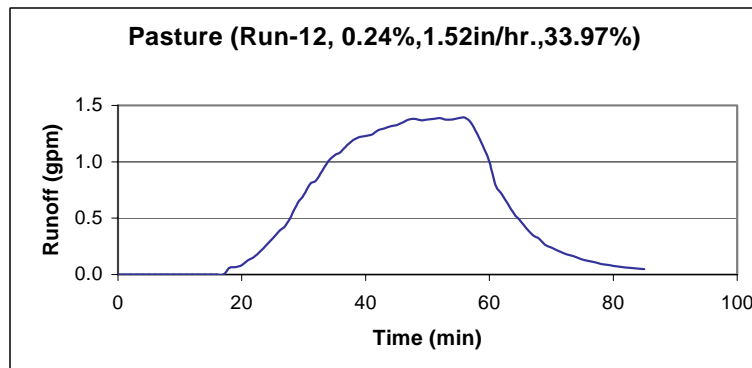

Figure E.5 Rainfall test on pasture (test 5)
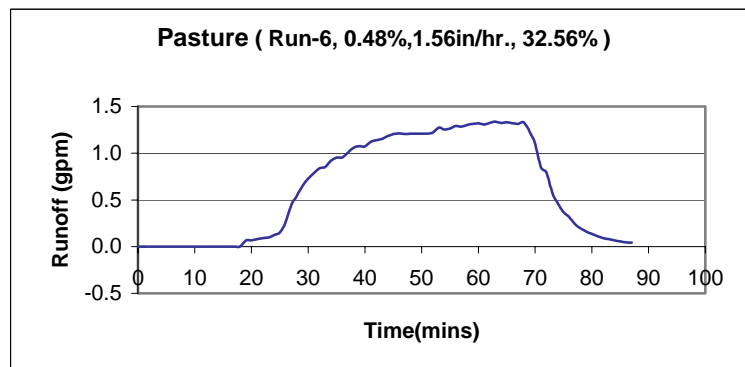
Figure E.6 Rainfall test on pasture (test 6)
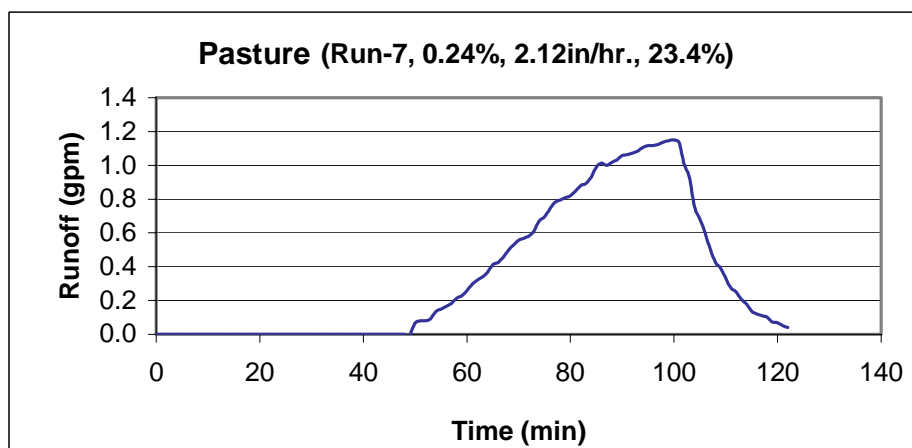
Figure E.7 Rainfall test on pasture (test 7)

Figure E.8 Rainfall test on pasture (test 8)
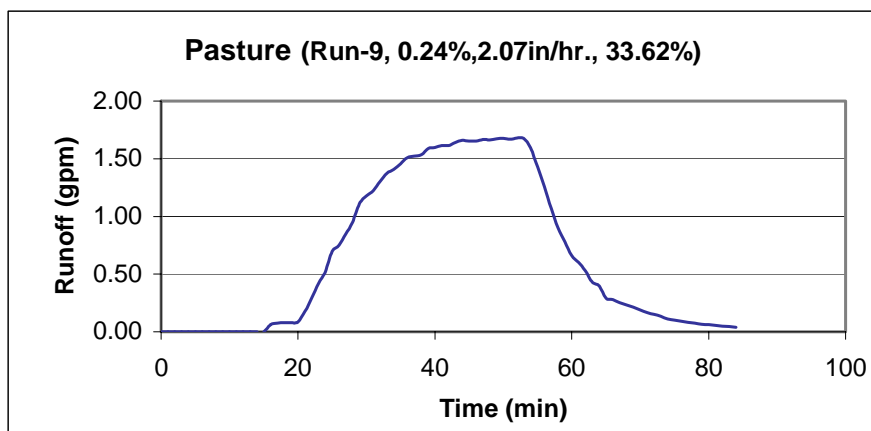
Figure E.9 Rainfall test on pasture (test 9)
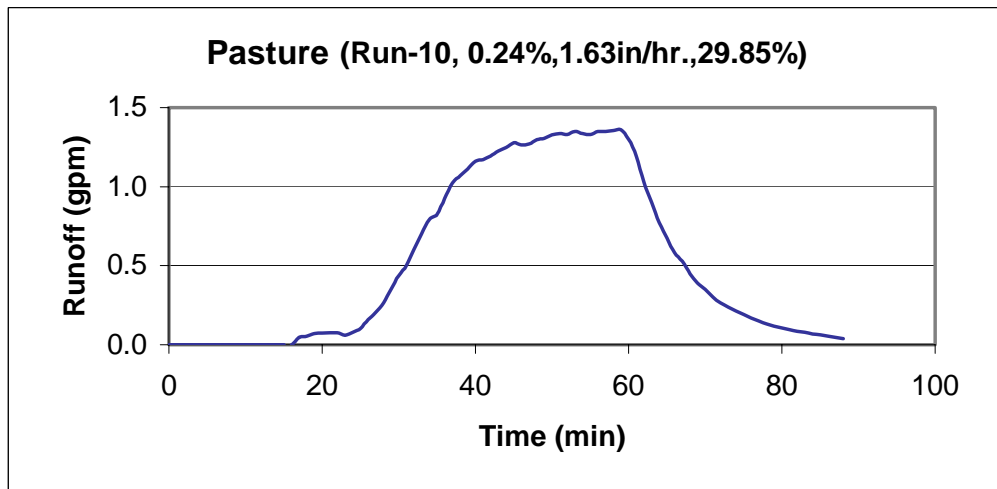
Figure E.10 Rainfall test on pasture (test 10)
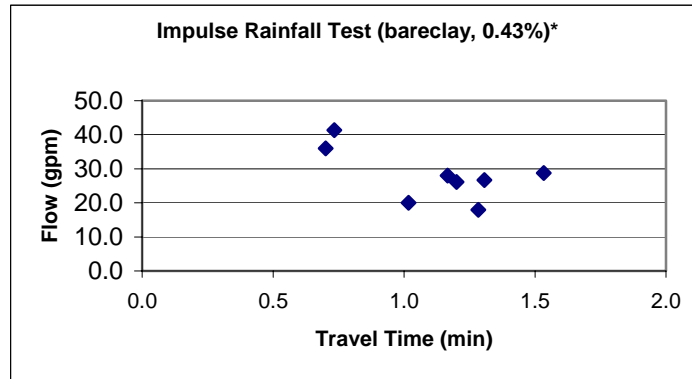

Figure E.11 Rainfall test on pasture (test 11)

Figure E.12 Rainfall test on pasture (test 12)

Impulse Rainfall Test (bareclay, 0.43%)*

* (surface type, surface slope)

Figure F.1 Impulse runoff test on bare clay plot 1 (8 tests)

Impulse rainfall Test (bareclay, 0.42%)
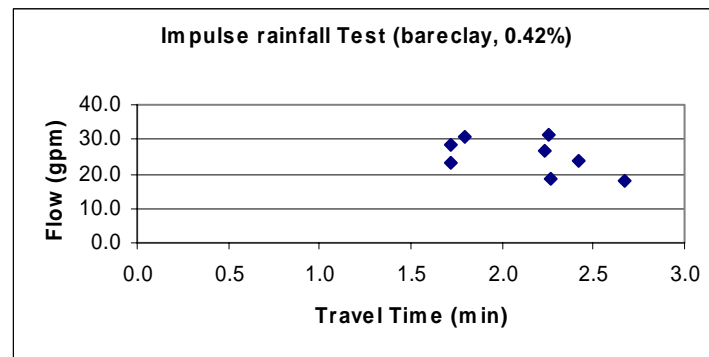
Figure F.2 Impulse runoff test on bare clay plot 2 (7 tests)

Impulse runoff test (asphalt, 0.35%)*
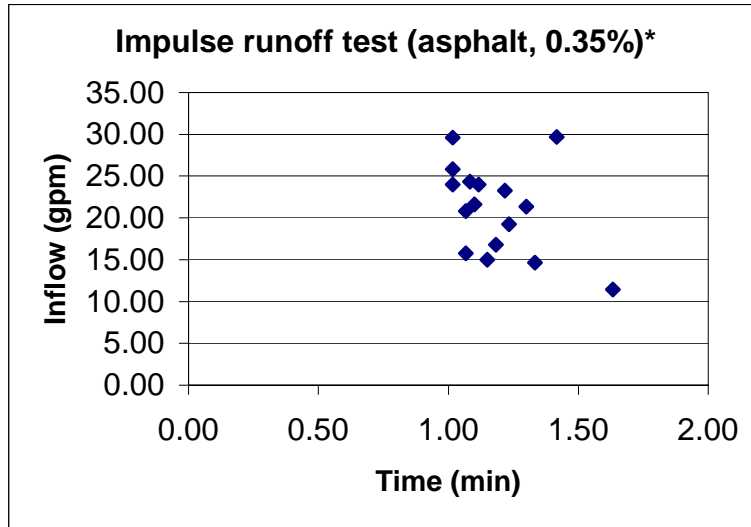
* (surface type, surface slope)

Figure G.1 Impulse runoff test on asphalt (16 tests)
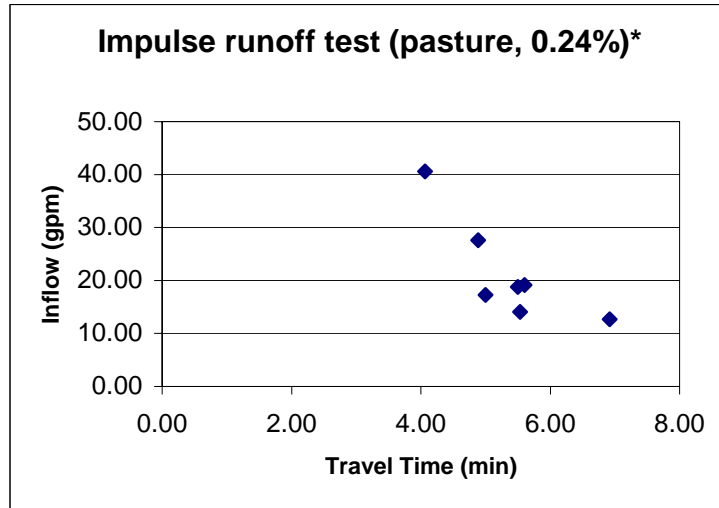
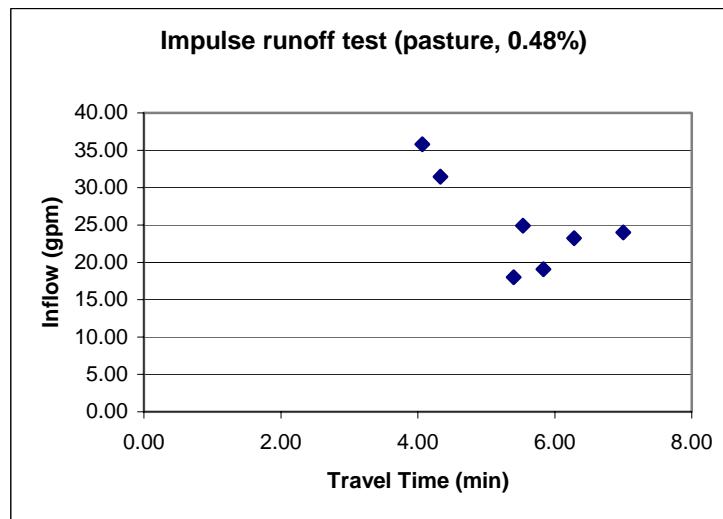Figure H.1 Impulse runoff test on pasture plot 1 (7 tests)

Figure H.2 Impulse runoff test on pasture plot 2 (7 tests)